AD NUMBER

AD477910

NEW LIMITATION CHANGE

TO

Approved for public release, distribution unlimited

FROM

Distribution authorized to U.S. Gov't. agencies and their contractors; Administrative/Operational Use; NOV 1964. Other requests shall be referred to Army Transportation Research Command, Fort Eustis, VA.

AUTHORITY

USAAMRDL ltr 23 Jun 1971

U. S. ARMY

TRANSPORTATION RESEARCH COMMAND
FORT EUSTIS, VIRGINIA

(6) PRELIMINARY FLIGHT TEST DATA.

XH-51A RIGID ROTOR HIGH SPEED FLIGHT PROGRAM.

(9) INTERIM REP[redacted]T, NO. 7

(11) NOV[redacted]964, (12) 36p.

042 200

The information contained herein has been reproduced to disseminate to Government and industry, as rapidly as possible, current data vital to Army rotary-wing progress and objectives. In this respect, it is emphasized that the data, although measured flight data, are preliminary; therefore, the contents of this document are subject to revision.

SUMMARY

This report summarizes the flight test results of the Phase III four-bladed rotor testing on the XH-51A "rigid rotor" helicopter. The object of Phase III was to evaluate the four-blade rotor in comparison with the three-blade rotor. Ground tests commenced on 13 July 1964 with the first flight on 21 July 1964. The phase was terminated on 3 October 1964 after 49 flights and 14.9 flight hours.

Results and Discussion

General

Two problems were apparent as a result of early flights, blade stresses and vibration level - both were high. At this stage, the transmission was in soft suspension in pitch only with a spring rate of 14,400 pounds/inch; vertically and laterally the mount was solid. The fuselage vibration problem was dominantly 4P; it was considered that this resulted from the second and third harmonics of blade natural flapping frequency which were close to 3P and 5P. The 3P and 5P rotating inputs resulted in a 4P shaft oscillation which was transmitted to the fuselage. The fuselage responds rather readily to frequencies in this range. The transmission suspension was varied incrementally to tune it to a point of minimum transmissability; this approach had not been completed at the close of Phase III. Additionally, experimental moves were made towards cutting down the input by reducing the blade natural flapping frequencies. The configuration at the termination of the phase, resulting from these two approaches, incorporated a 13-pound weight at station 6.0 on each of the four blades and the transmission soft mounted in pitch, roll, and vertically. Blade stresses were reduced to within the infinite life level and vibration, although unacceptable from a production viewpoint, was also considerably reduced.

Apart from the vibration level, no flying qualities problems were encountered. A marked increase in the Phase III flight envelope was achieved, 2.5 g being demonstrated from 0 to 120 knots CAS and a speed of 180 knots IAS flown in a shallow dive.

Phase III employed four blades of the same design used on the three-blade rotor, the hub blade attachment geometry was modified compared with that employed in the Phase II flying. The only significant problem apparent at the close of Phase III was fuselage vibration, none of the stability problems encountered with the three-blade rotor existed and stress levels, subject to fatigue test confirmation, indicate infinite life for the hub. With the reduction of the vibration level to within normal limits, a substantial speed envelope expansion should be possible. The phase is considered a considerable success in that a marked increase in flight envelope was demonstrated, no stability problems existed, and no problems considered insurmountable were encountered. The stability characteristics confirmed the advisability of the choice of the four-blade rotor for the compound configuration.

Configuration

Four-blade rotor - The blade design was that employed during Phase II, the three-blade rotor; however, the blade hub attachment was modified. The cone angle built into the hub was increased from 2.8 degrees to 3.2 degrees.

Main rotor gearbox suspension varied as described.
Tailplane angle of incidence $-5\frac{1}{2}^{o}$ through test 271 and -3^{o} thereafter.
Blade weights 13 pounds each, fitted to each main rotor blade at station 6.0 for test 352 and remained on thereafter.
Four-arm gyro 7.3 slug ft^2.
Arm incidence 30 degrees.

Structures

Structural loads recorded during the program included main rotor hub and blades, gyro control arms, main rotor pitch link, tail rotor and tailplane loads. An incremental approach was employed during the tests, flight records being examined prior to further envelope expansion.

Figures 1 and 2 compare Phase II and III flight envelopes. At a C.G. of 1.5" forward, the envelope is substantially 2.5 to 0.2 g up to 120 knots CAS with reducing normal acceleration out to 165 knots CAS. The aft envelope was opened up in only three or four flights and no specific attempt was made to exceed the Phase II envelope. While it is felt that there would be little point in extending the hover beyond the 0.15 to 2.7 g demonstrated, no structural, performance, or stability limits were encountered in forward flight.

Rotor Stresses

A review of all structural data indicates that hub station 7.0 is the critical fatigue section of the rotor. It consists of three steel laminations bonded and bolted together. Assuming a stress concentration of 3, the endurange limit stress is 26,000 psi. The strain calibrations were effected in terms of bending moment rather than stress because the bending moment curve along the span of hub and blade is predictable. The conversion of bending moment to stress at station 7.0 is as follows:

Flapwise bending	Station 6.0 moment x 1.42 = station 7.0 stress
Chordwise bending	Station 6.0 moment x 1.152 = station 7.0 stress

Figure 3 shows that during the initial flights, the chordwise bending stress was 40 percent lower than that in the three-blade, but the flapping stress was up by 80 to 90 percent. At this stage, the vibration was very high and a series of changes in transmission suspension springs was initiated to reduce both vibration and stress. The pitch spring rate was varied first; the range covered was 6,400 pounds/inch to solid while both vertical and lateral remained solid. From the structural loads and vibration results 11,000 pounds/inch was selected as the pitch spring rate to be held constant during vertical spring variations. The vertical range covered was from solid down to 4,000 pounds/inch and 6,000 pounds/inch was selected from the results.

An analysis of the flapwise bending at station 6.0 during forward flight and flare showed considerable 3P and 5P content superimposed on the 1P. Note, 1P is main rotor rotational frequency, normally 5.9P cps (100T), 3P is 3 times rotor frequency, etc. The second and third harmonic blade natural flap bending frequencies were slightly below the 3P and 5P forcing frequencies. Tests conducted at 95 percent, 100 percent, and 105 percent illustrated the diminishing response of the blade as the forcing frequency was increased and separated from the natural. The 3P and 5P bending moments were reduced by approximately 45 and 55 percent respectively. The reduction of the blade natural frequencies had a similar effect; at 100 knots, the 3P bending moment was reduced from 4,090 inch pounds to 2,400 inch pounds and the 5P from 1,960 inch pounds to 740 inch pounds. In reducing these moments, the weights reduced the 3P and 5P driving forces which produced the 4P pitching and rolling moment into the fuselage. The vibration benefited to a minimum degree.

To reduce the 4P moment further, a transmission lateral spring was introduced with a rate of 19,000 pounds/inch; it did reduce the cabin vibration to a small degree, but did not affect the structural loads.

Records showed a 1P flapping component increasing with speed at high speed and producing a nose down moment and indicating that a reduction of tailplane negative incidence would be of value in reducing the total bending moment. The tailplane incidence was changed from $-5\frac{1}{2}^{\circ}$ to -3° for test 228. The change in slope of the flapwise bending moment curve between figures 4 and 5 at high speed is attributable to this change.

Figures 6 and 7 illustrate the affect of normal accelration on the flapwise bending moment at station 6.0 at two centers of gravity. The average moment increased towards up flapping with increasing load factor due to lift on the rotor blade. Down flapping was recorded at 1.0 g due to the fact that the blade line was below the cone angle built into the hub. Zero moment was recorded when the blade at this station lined up with the hub cone angle. The smaller built-in cone angle on the three-blade rotor and the 30 percent greater lift per blade resulted in the different intercept shown in the graphs. The Phase III flapping cyclic stresses, figure 7, at the aft C.G. were of the order of 10 percent lower than those at a mid-C.G. on Phase II. At the forward C.G., figure 6, they were about 30 percent lower than the Phase II mid-C.G. Chordwise average and cyclic moments in maneuver were 50 percent lower than with the three-blade rotor except at high load factors where the reduction in average moment was about 10 percent. The cyclic flapwise and chordwise stresses at station 6.0 are the maximum that occurred during the maneuvers and do not necessarily coincide with the maximum load factor.

The spanwise bending moment distribution in high speed level flight, descent, and in maneuver are shown in figures 10 through 15.

Vibration

Vibration level in the cabin was measured for speeds up to 132 knots CAS in level flight and to 165 knots CAS in a descent. Tri-axis (vertical, fore and aft, lateral) measurements were made on the cabin floor at the pilot's seat. Vibration data in the 3 axes is plotted versus airspeed (CAS), figure 16.

The analysis of vibration for the various configuration was carried out in conjunction with the structural loads, because they were in most cases a function of each other. The comparison with the three-blade data is obvious, but it must be pointed out that the three-blade data represents only the soft cabin configuration. The high vibration level remaining at the termination of Phase III was the only problem of any significance and was the factor which limited the speeds attainable under this contract.

Stability

No adverse stability characteristics were recorded at any time throughout the Phase III flying. There was a tendency for the static longitudinal stability to become neutral at high speed and some cyclic cross-coupling existed. The correction of the cross-coupling would have improved the stability which could have been made further positive by aerodynamic shaping of the gyro arms. For the purposes of the program, neither the stability nor the coupling warranted corrective action.

The cyclic control to trim is shown in figures 17 and 19 in terms of control position and maximum blade incidence. Figure 18 shows the results of constant collective static stick fixed and free longitudinal stability measurements.

Figures 20 and 21 illustrate the longitudinal and lateral control power and 22 compares Phase II and Phase III results. The lateral control power was increased by 14 percent to 12.0 degrees/second-inch and in both phases and was independent of speed. Longitudinally, the 20 to 25 percent increase apparent at the lower airspeeds decreased with speed to become zero at about 110 knots IAS. The data was obtained from longitudinal step inputs in the hover and at 70 and 110 knots IAS. The time histories showed compliance with MIL-H-8501A in that the angular velocity was in the proper direction within 0.2 seconds of the control displacement and the point of inflection of normal acceleration occurred within 1.0 second of the control displacement.

The stick force per g plots in figures 23, 24, and 25 illustrate the greatest single improvement of the four-blade rotor relative to the three-blade rotor. No pitch up, nor any tendency for the stick force/g to be other than positive was experienced during Phase III. The stick force/g has improved 150 to 200 percent, providing a high degree of confidence with regard to the anticipated outcome of maneuver tests at high airspeeds. An envelope of the bank angles flown during these maneuvers is presented in figure 26.

A number of entries and autorotations were affected in the range 80 to 120 knots CAS; the characteristics were normal and perfectly acceptable. The load factor to hold rotor speed presented in figure 27 stems from tests conducted to assist in the definition of the technique to be used following failure of the rotor engine on the compound helicopter.

Performance

Performance data presented in figure 29 is not representative of the four-bladed clean helicopter configuration in that at the time the tests were conducted, the blade weights were installed, and they represent a significant and unknown drag increment. The hover data presented in figure 28 is clean four-blade data.

DATA APPENDIX
INDEX

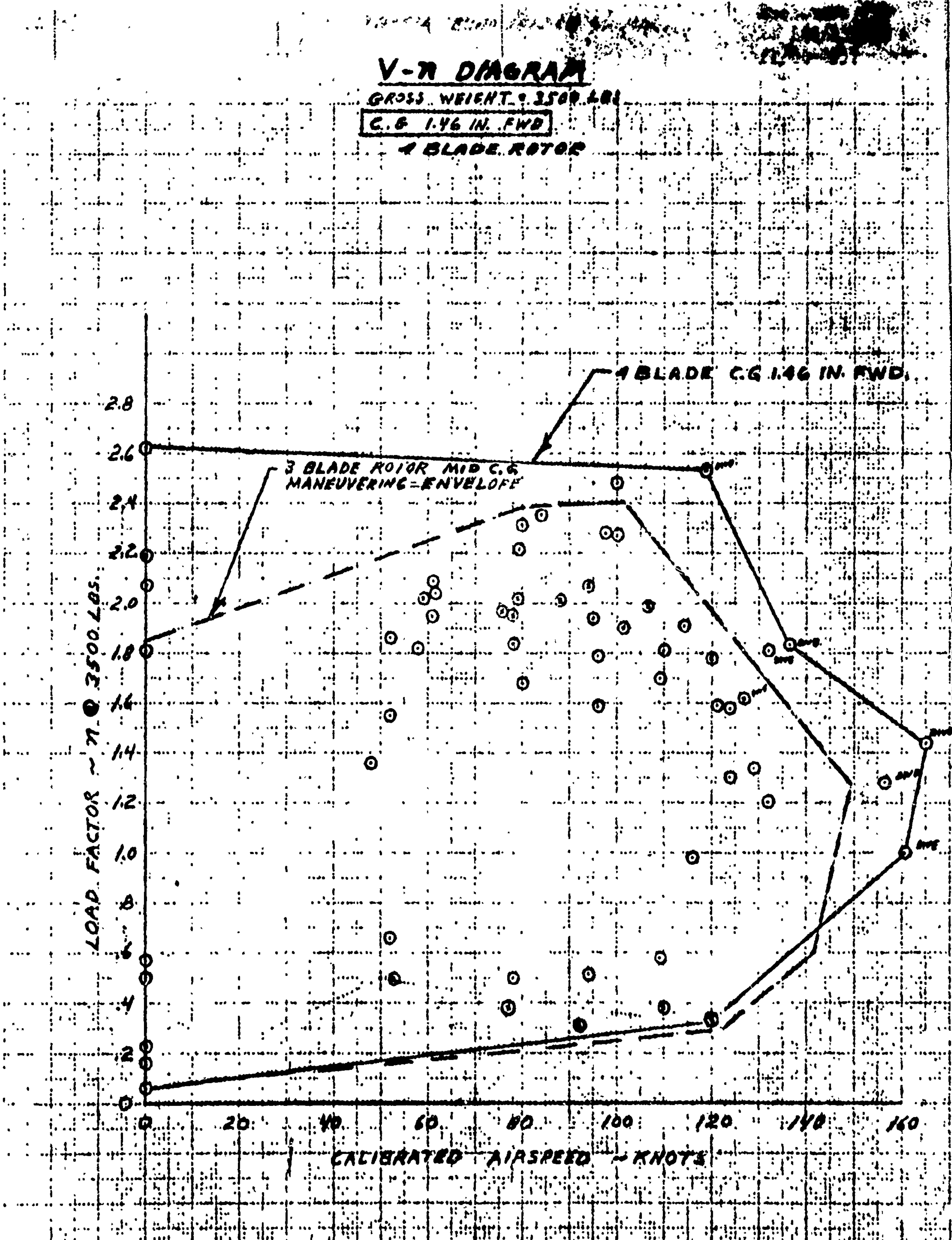

FORM 8879A

FLIGHT ENVELOPE C.G. 1.46" FWD.

S.F.61.1
FIG.1

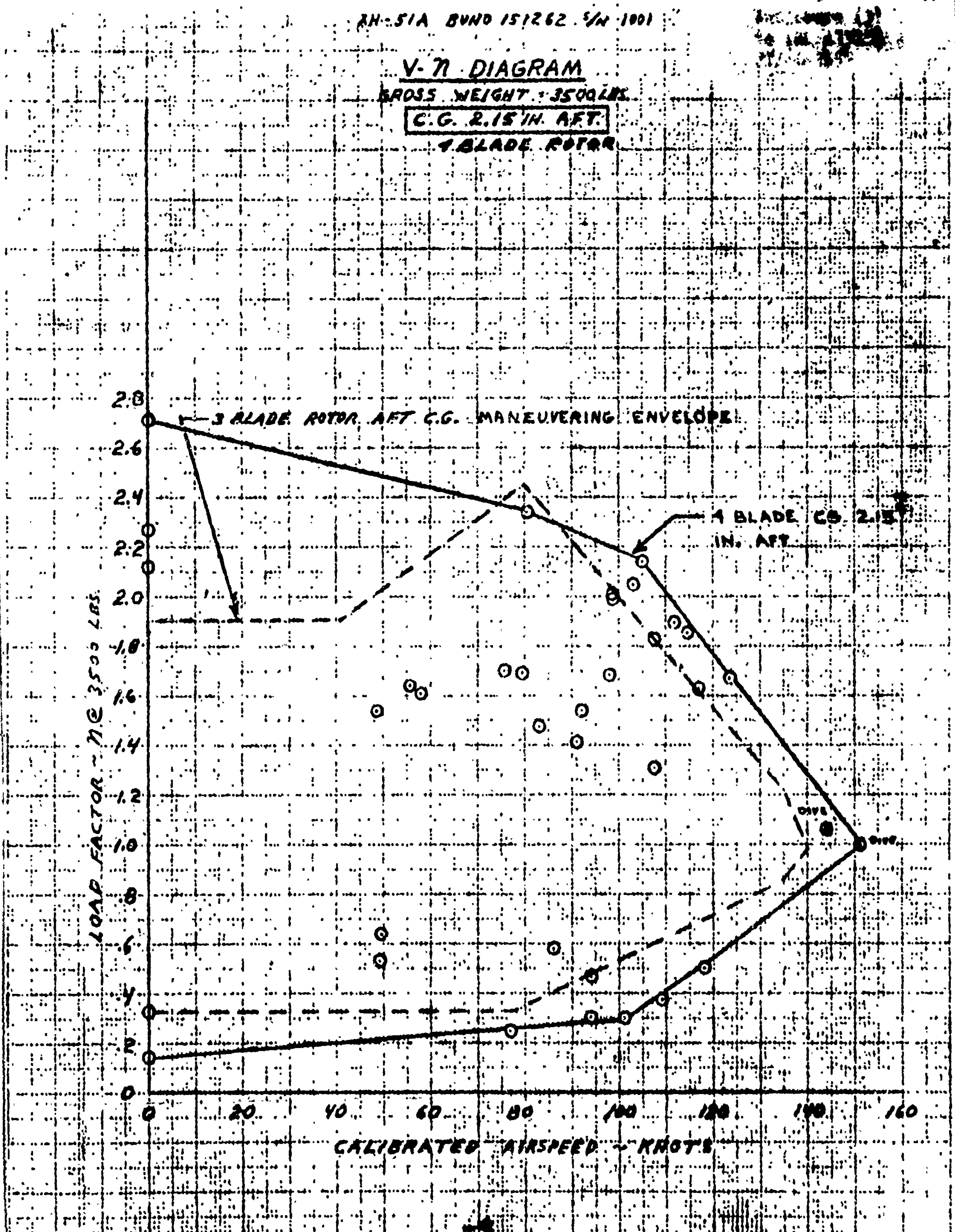

FLIGHT ENVELOPE C.G. 2.15" AFT

SF 60.1
FIG 2

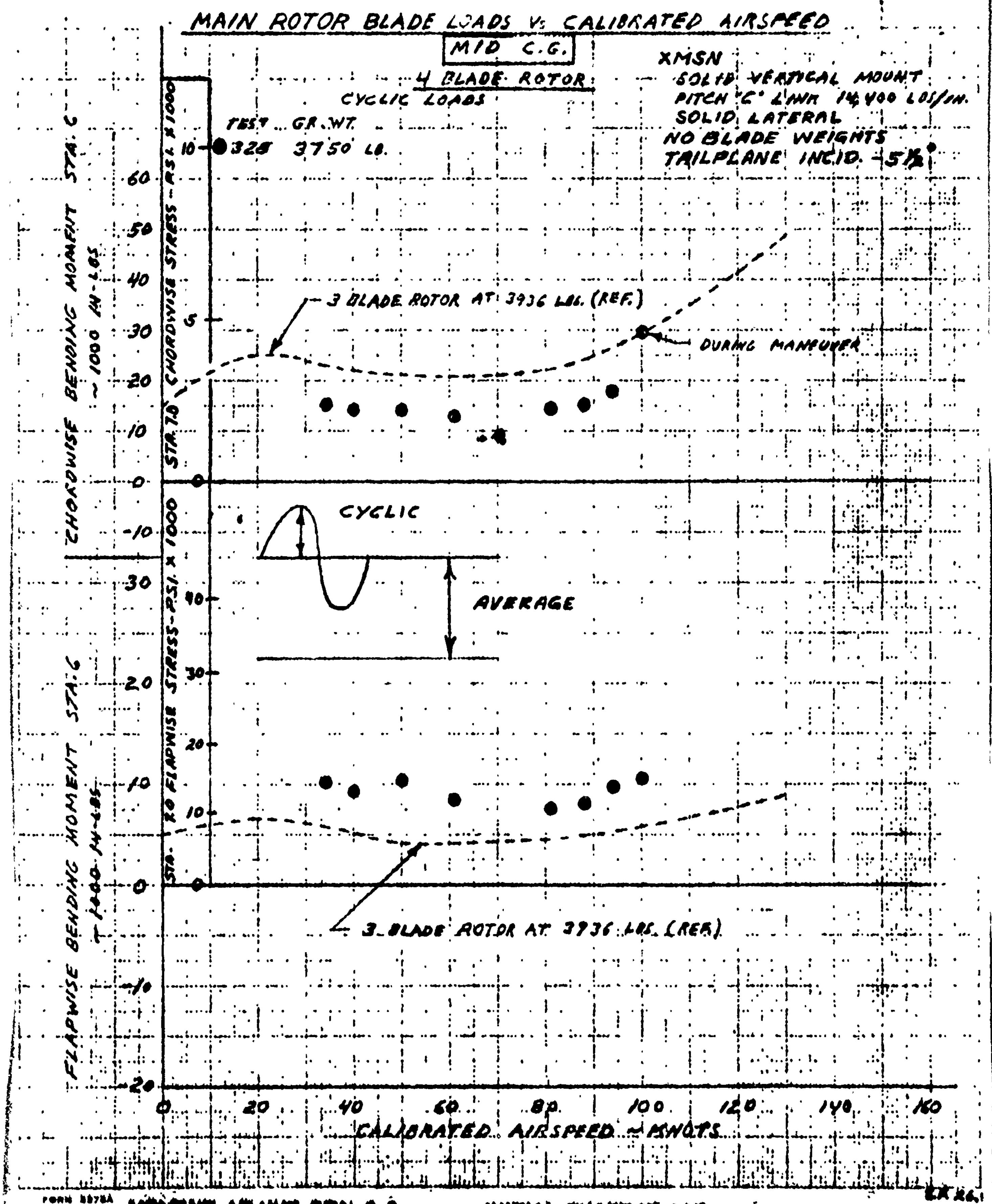

MOMENT AT HUB STA. 6.0 INITIAL PHASE III DATA FIG 3

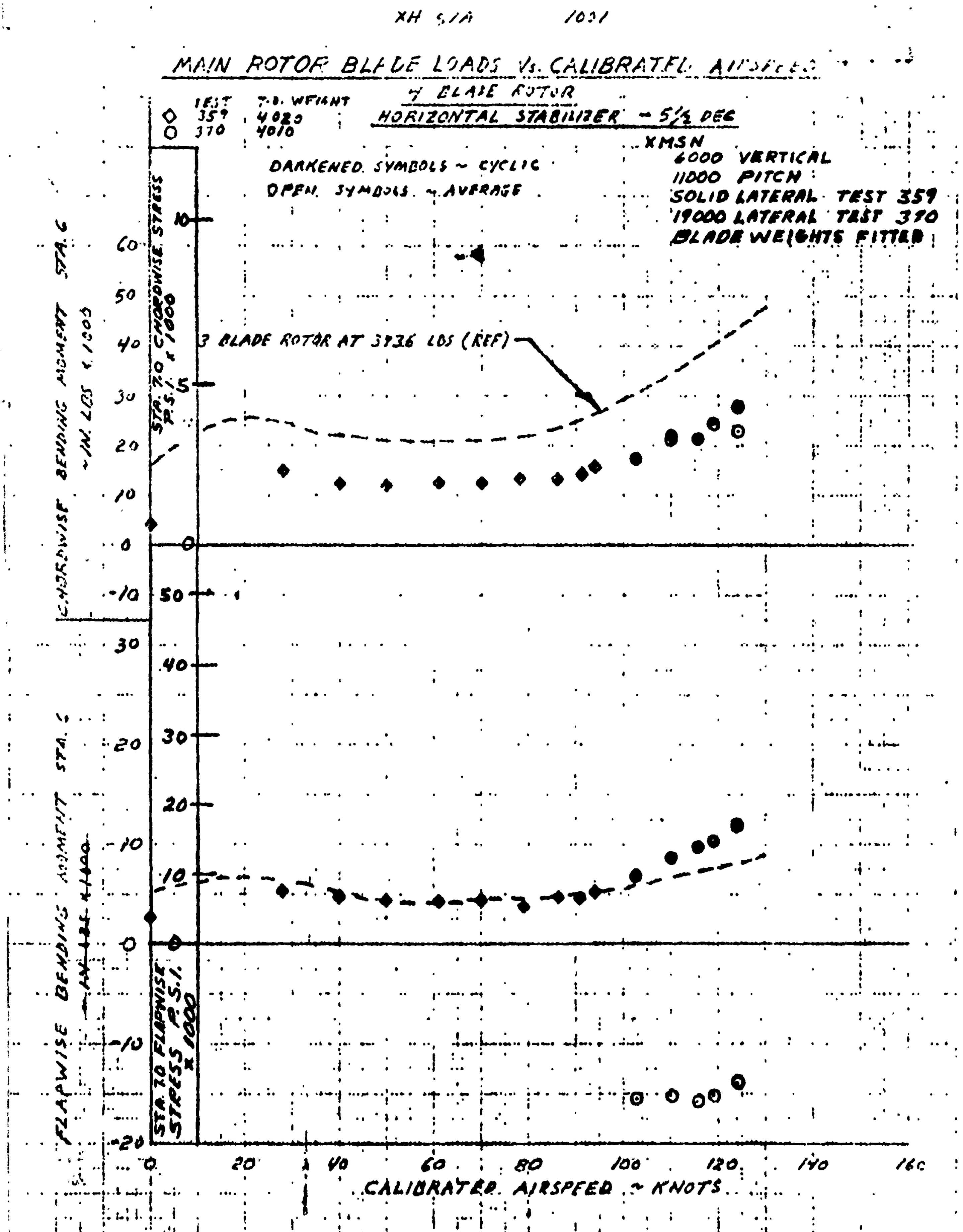

MOMENT AT HUB STA. 6.0 TRANSMISSION SUSPENSION MODIFIED
BLADE WEIGHTS INCORPORATED

SF. 51.1
FIG 4

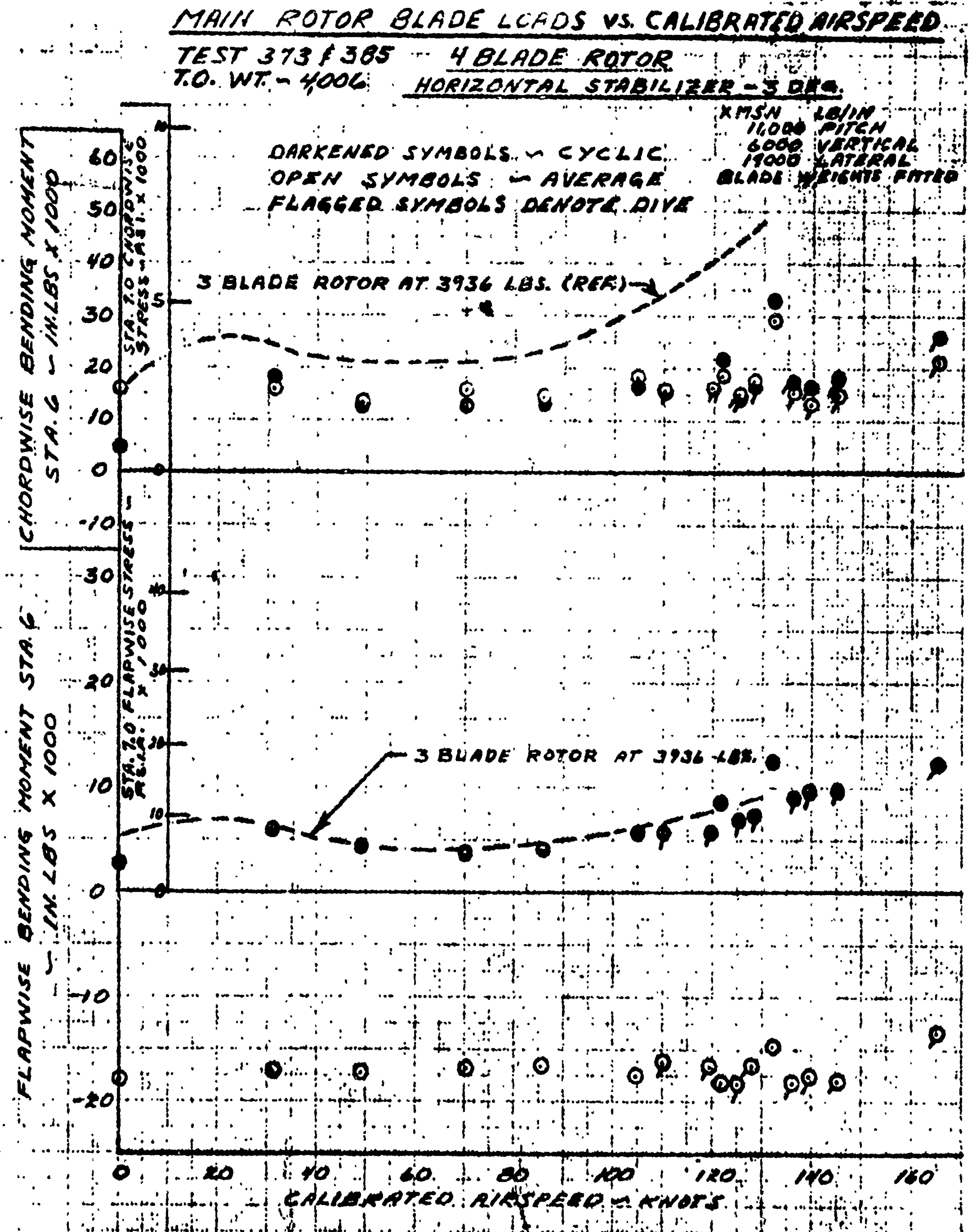

FORM 8270A

S.F.62.1

MOMENT AT HUB STA. 6.0 FINAL PHASE II CONFIG. TAILPLANE -3° FIG 5

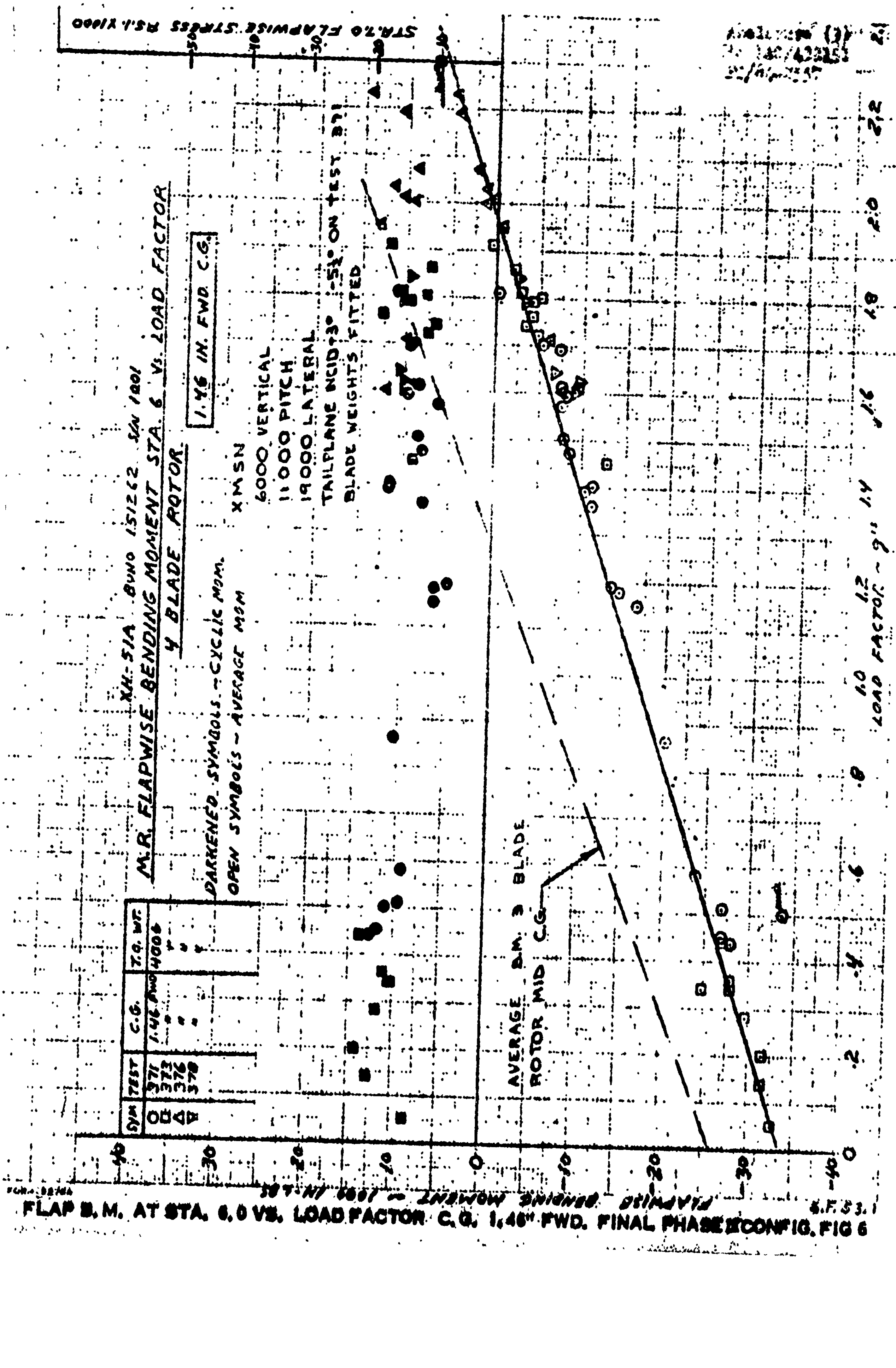

FLAP B.M. AT STA. 6.0 VS. LOAD FACTOR C.G. 1.46" FWD. FINAL PHASE CONFIG. FIG 6

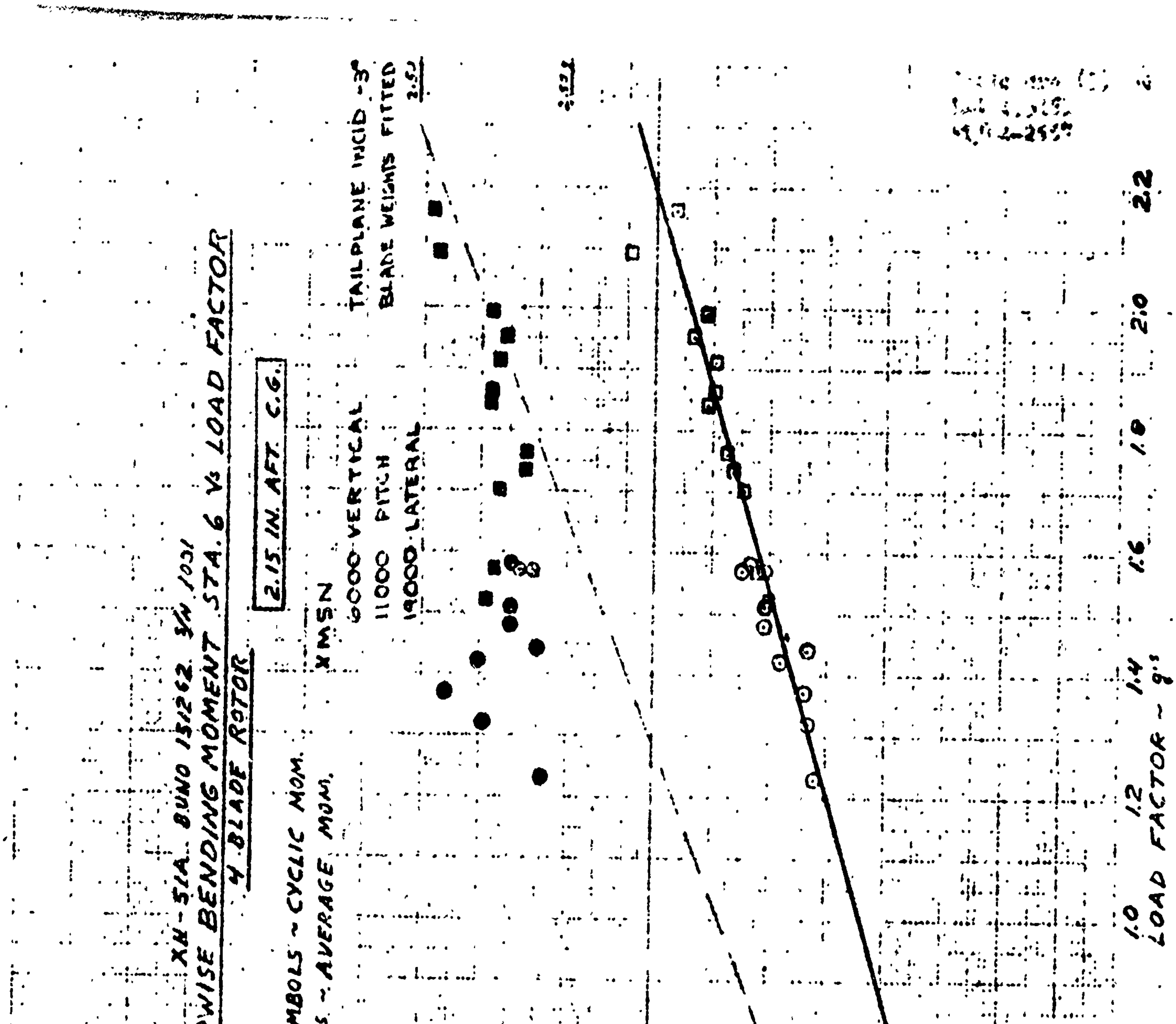

FLAP B.M. AT STA. 6.0 VS. LOAD FACTOR C.G. 2.15" AFT FINAL PHASE FIG 7

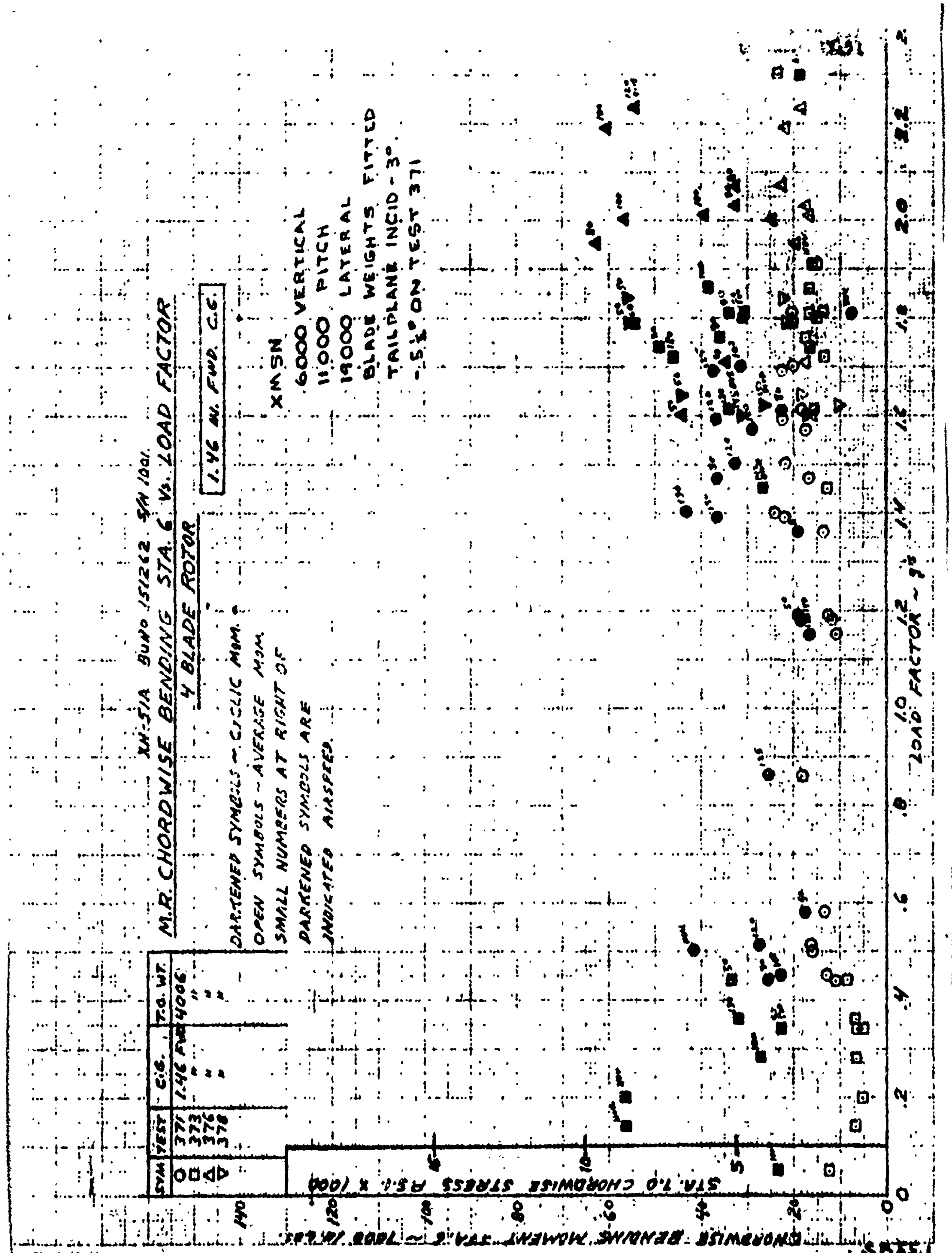

CHORD B. M. AT HUB STA. 6.0 VS. LOAD FACTOR C.G. 1.46" FWD

FINAL PHASE III CONFIG.

FIG 8

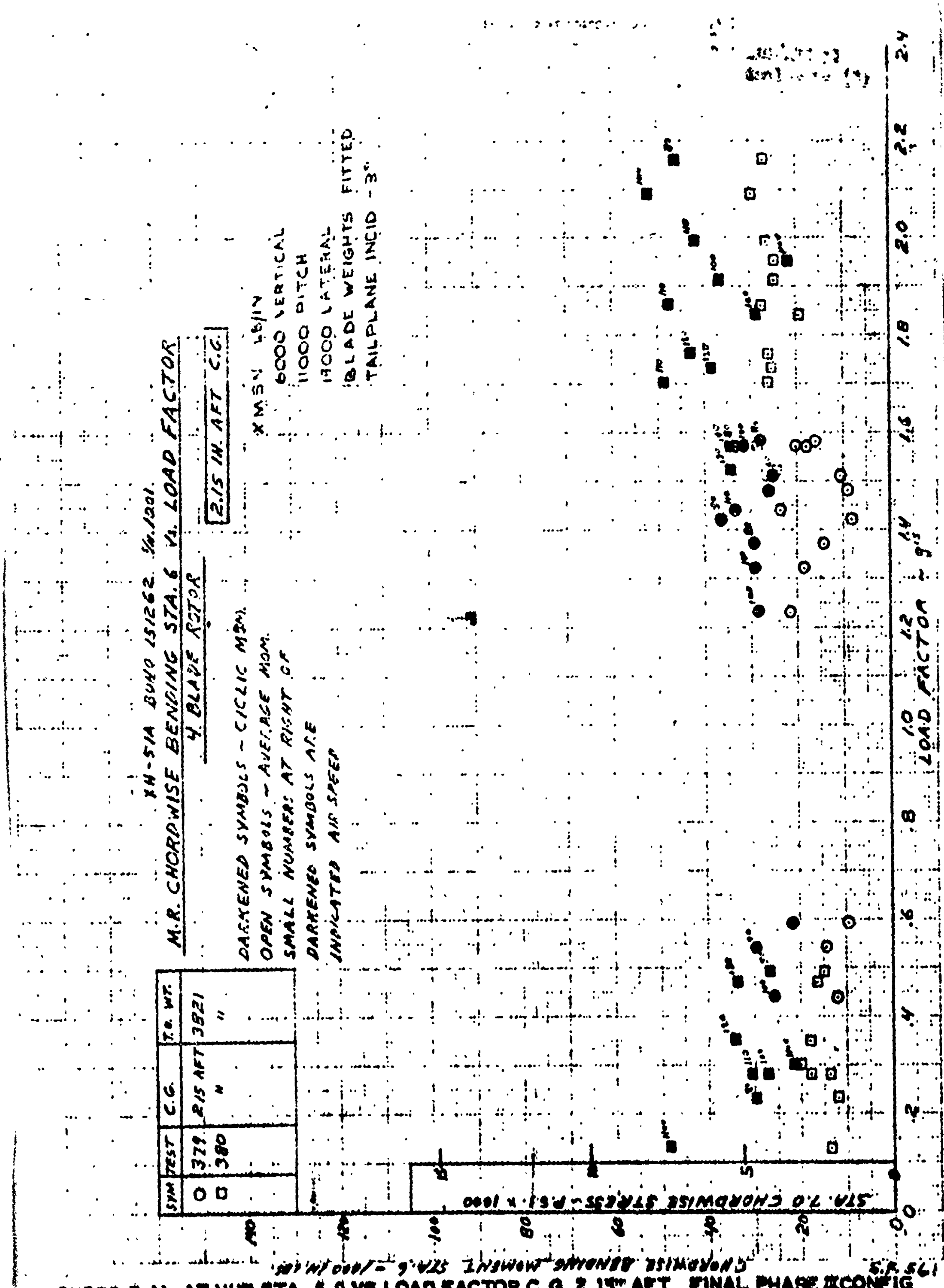

S.F. 561

CHORD B. M. AT HUB STA. 6.0 VS LOAD FACTOR C.G. 2.15" AFT FINAL PHASE II CONFIG

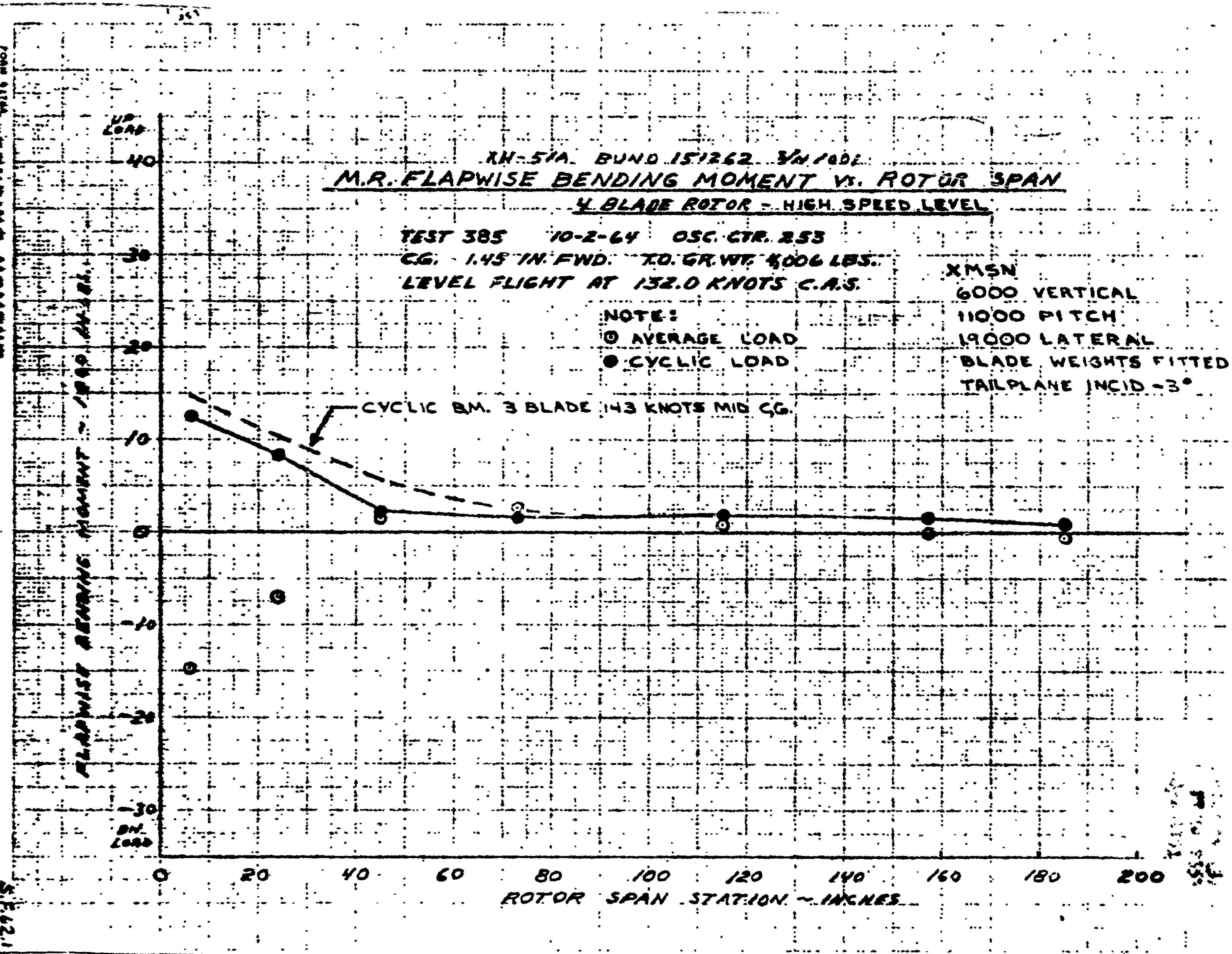

FLAPBENDING MOMENT VS. SPAN-LEVEL FLT. FINAL PHASE III CONFIG.

S.F.62.1

FIG 10

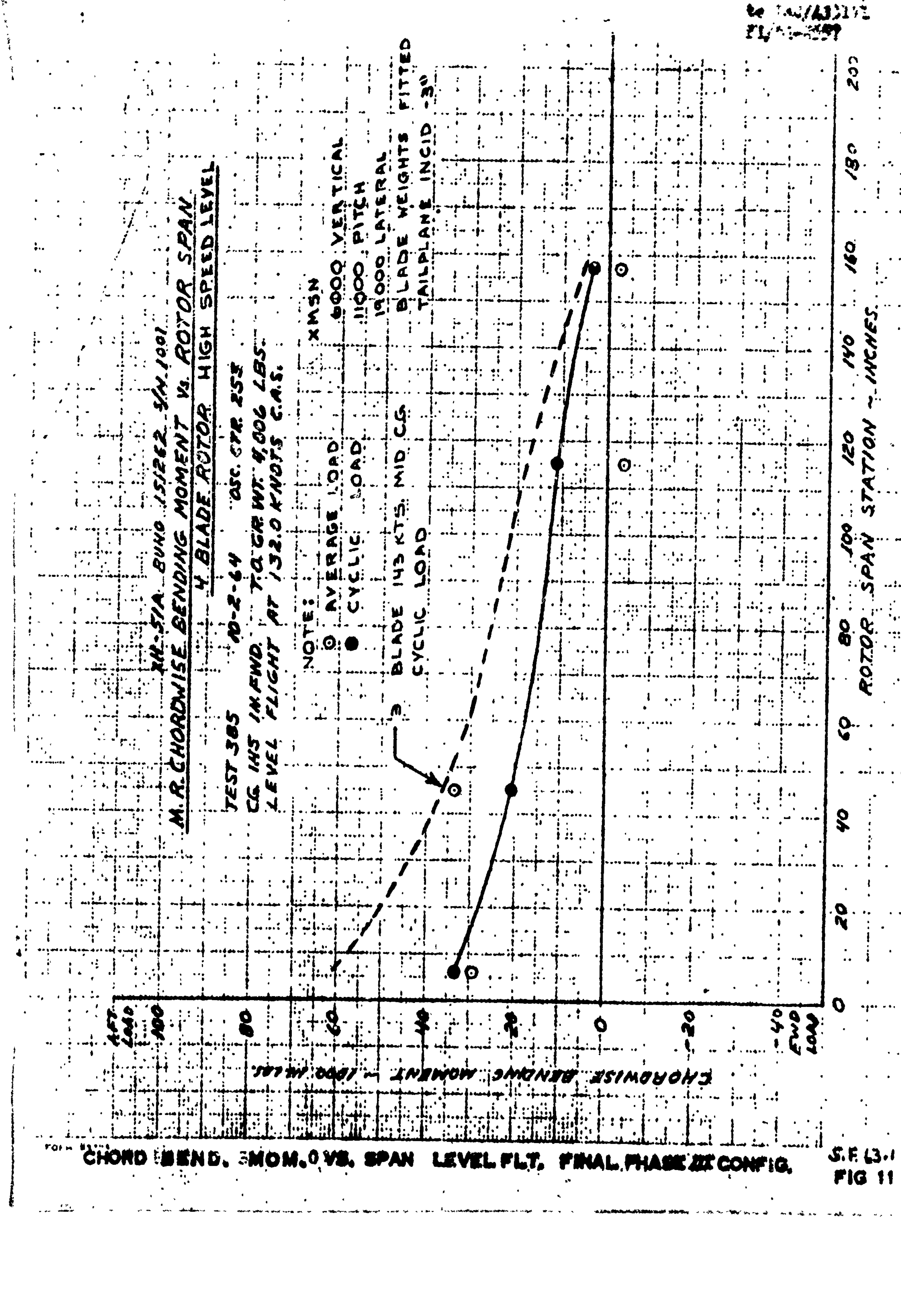

CHORD BEND. MOM. VS. SPAN LEVEL FLT. FINAL PHASE III CONFIG.

S.F. 63.1
FIG 11

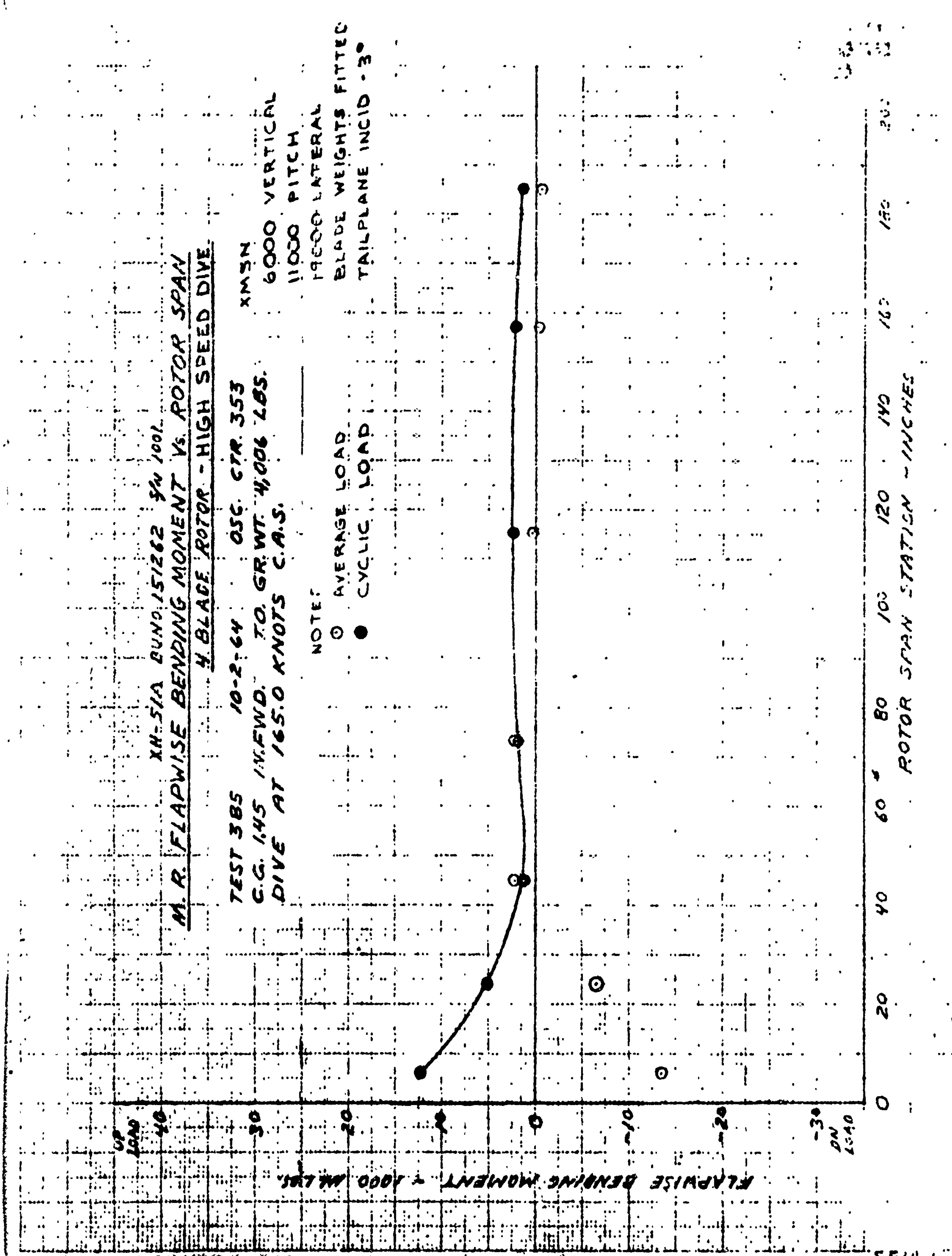

S.F.64-1

FLAP BENDING MOMENT VS. SPAN IN DIVE FINAL PHASE III CONFIG.

FIG 12

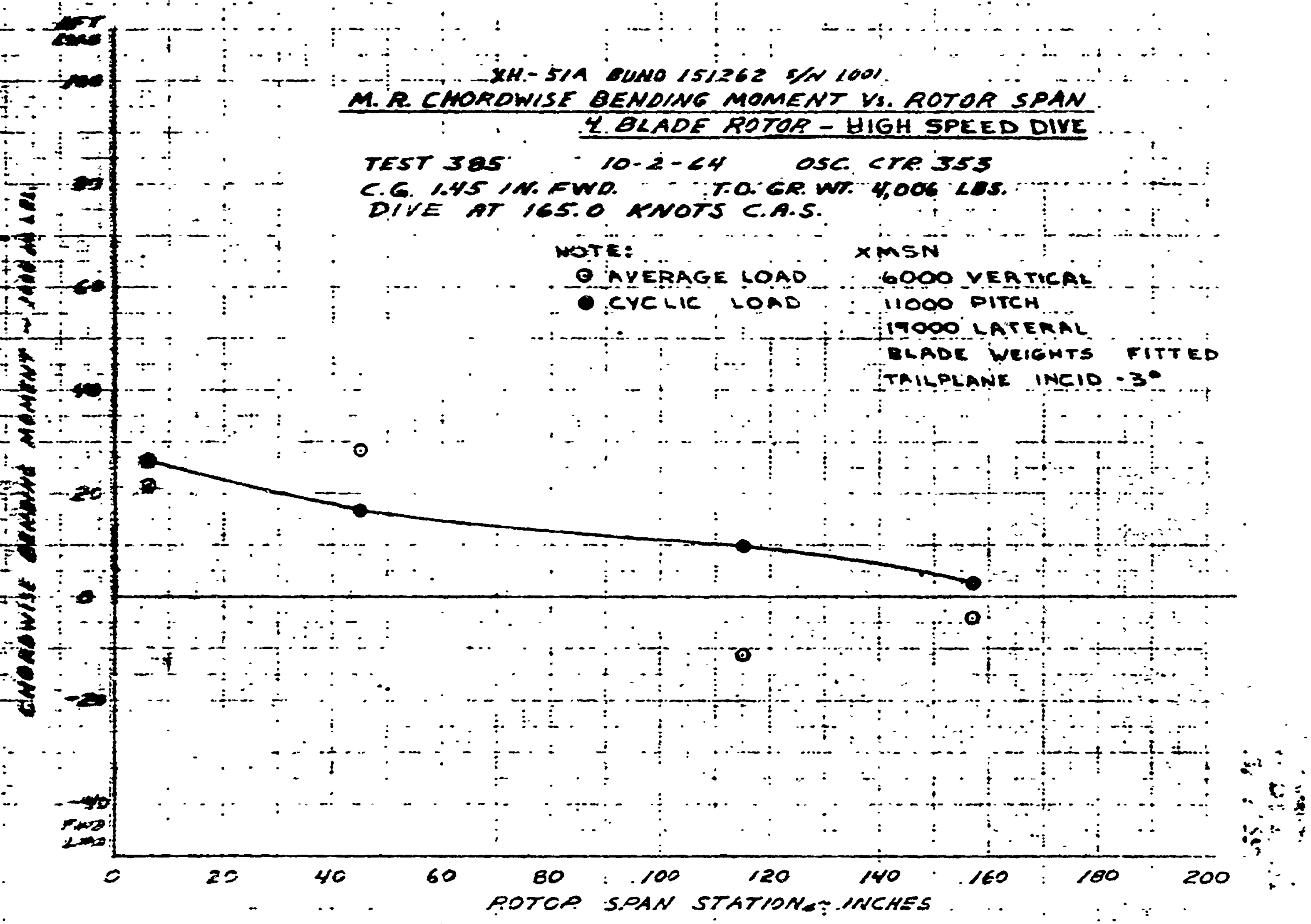

CHORD BENDING MOMENT VS. SPAN IN DIVE FINAL PHASE III CONFIG.

S.F.65.1
FIG 13

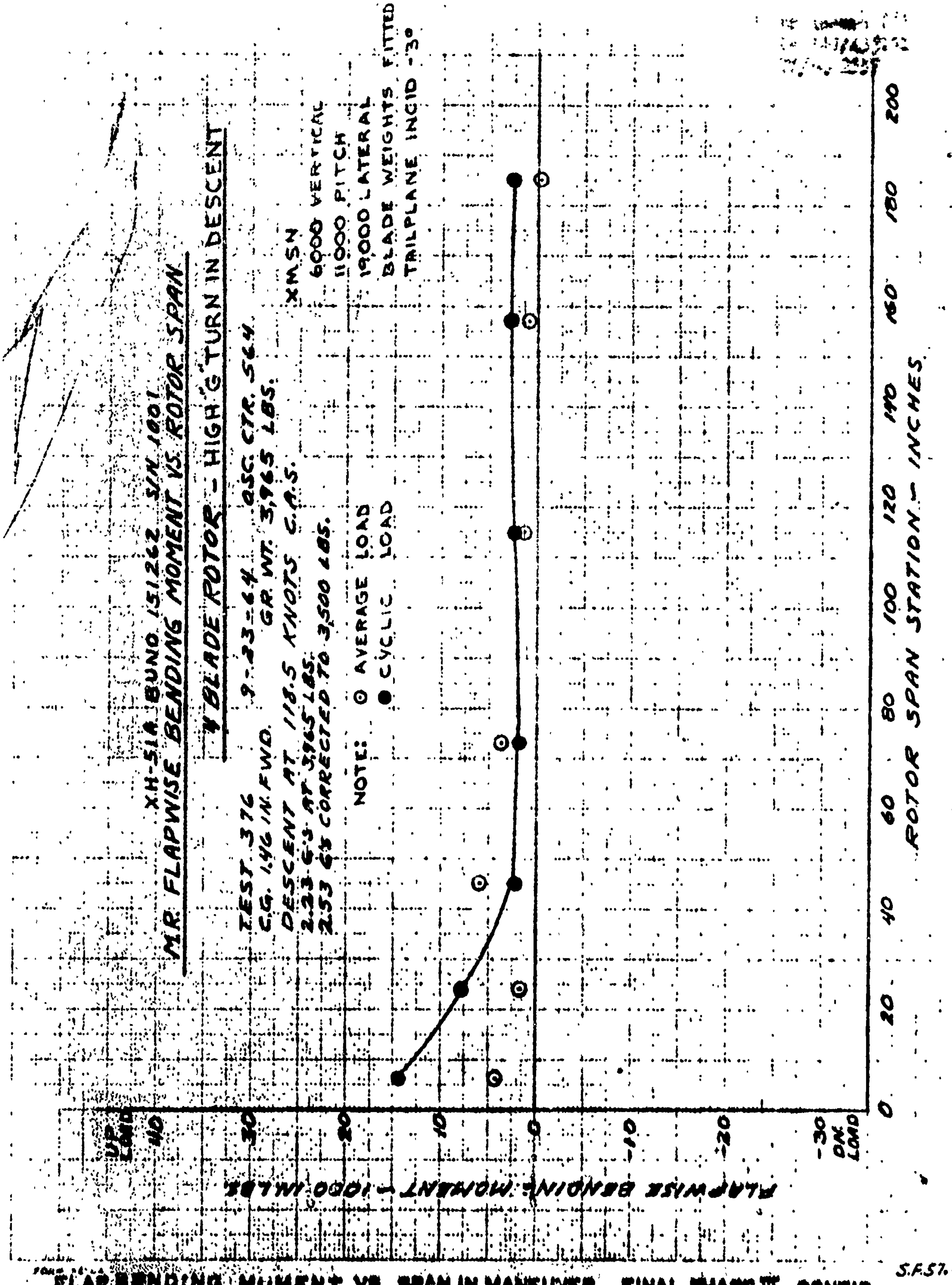

S.F.57.

FLAP BENDING MOMENT VS. SPAN IN MANEUVER FINAL PHASE III CONFIG. FIG 1

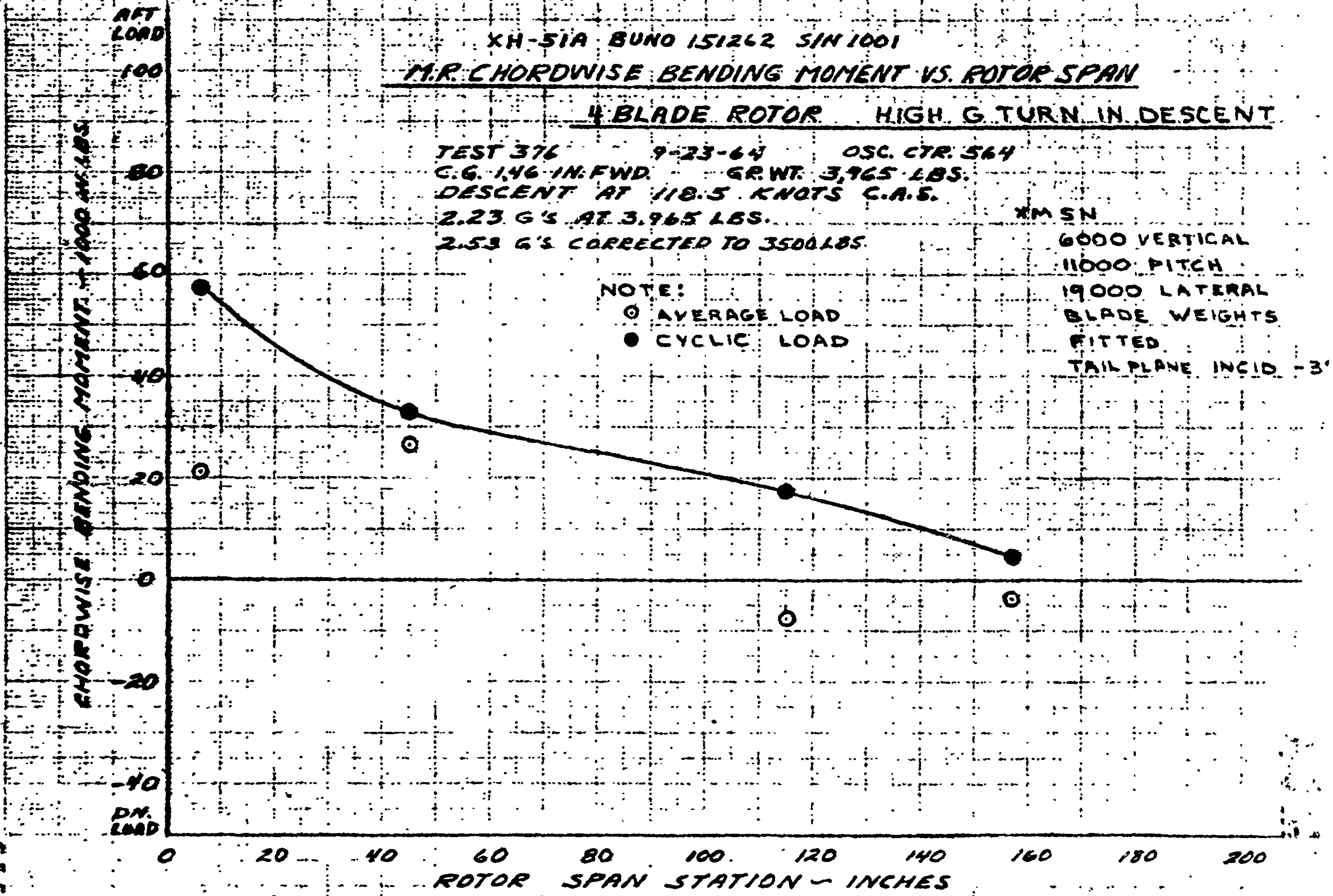

CHORD BENDING MOM. VS. SPAN IN MANEUVER FINAL PHASE II CONFIG.

E.F. 58.1
FIG 15

CABIN VIBRATIONS VS. CALIBRATED AIRSPEED

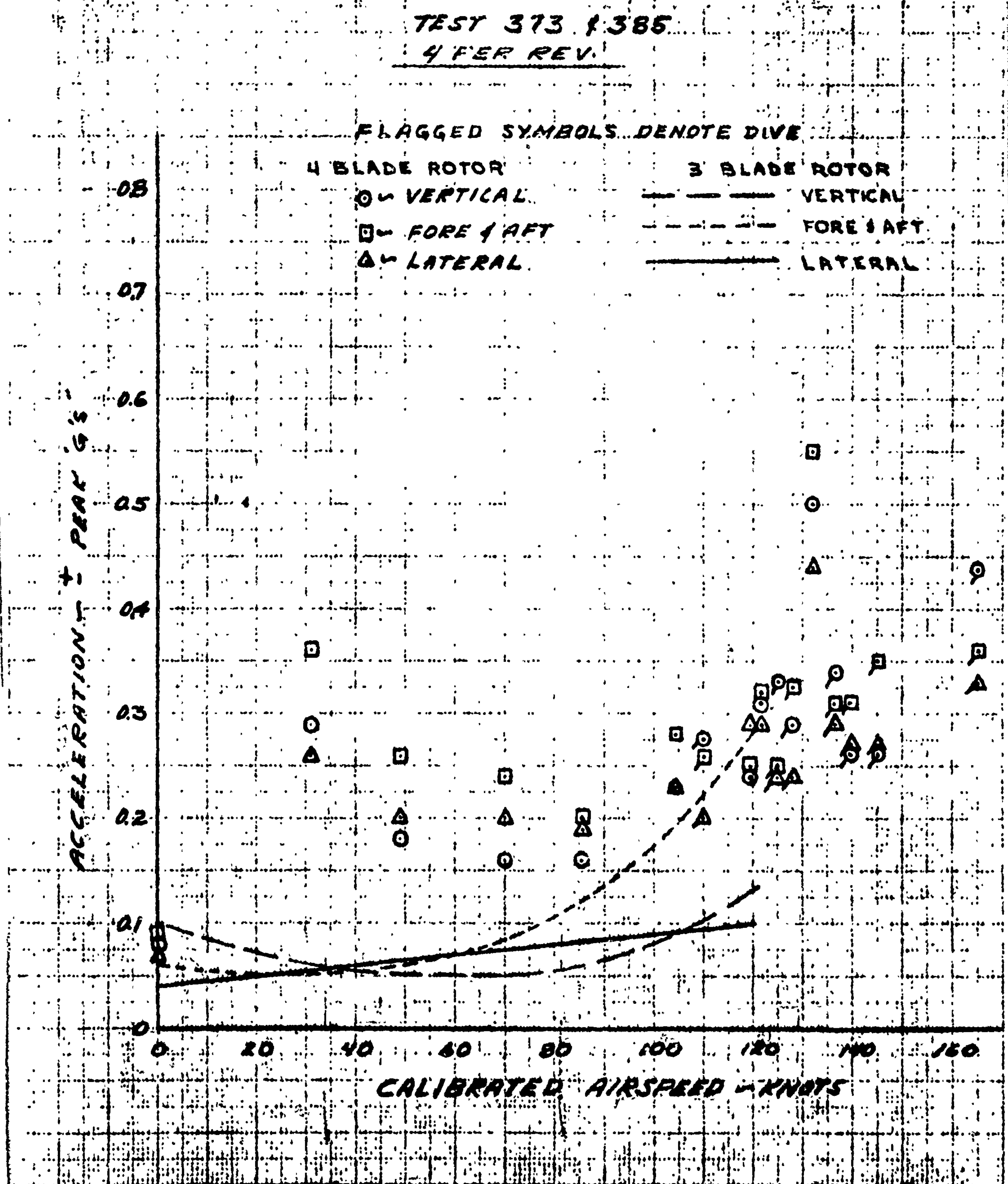

CABIN VIBRATION LEVEL. FINAL PHASE CONFIG.

S.F.59
FIG 16

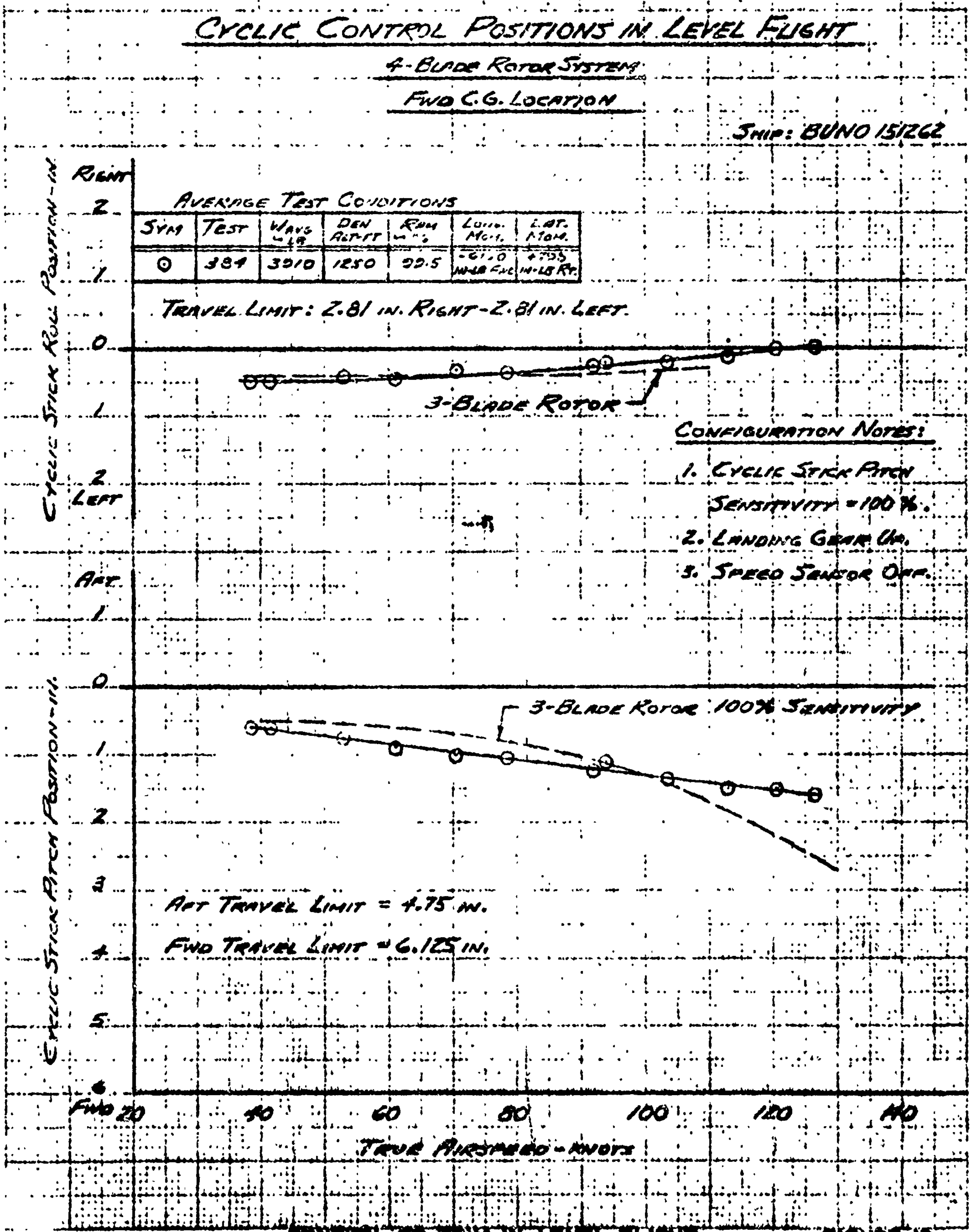

CONTROL TO TRIM IN LEVEL FLIGHT

FIGURE 17

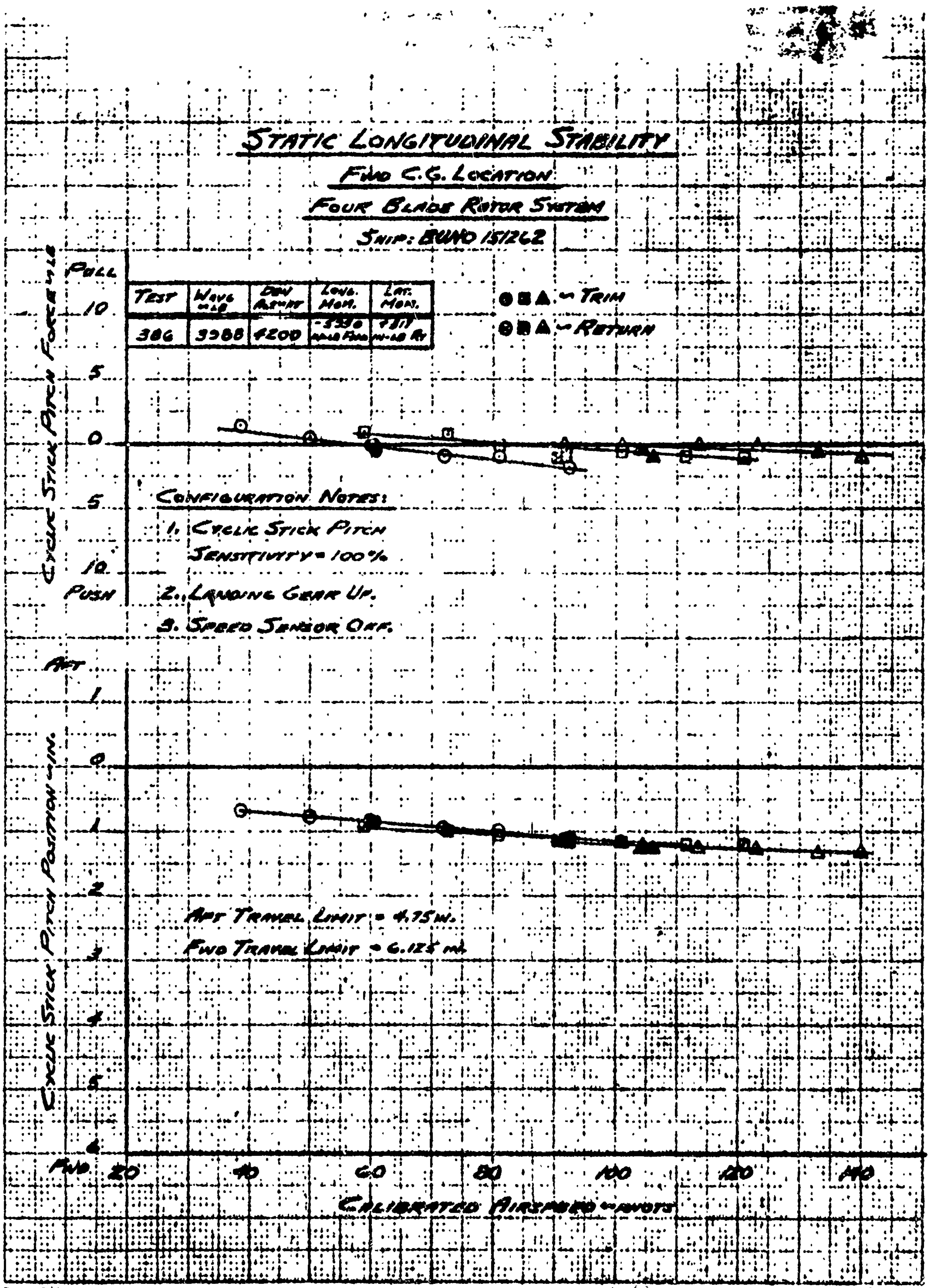

FORM 837C

CONSTANT COLLECTIVE STATIC LONGITUDINAL STABILITY (10W)

993A

FIGURE 18

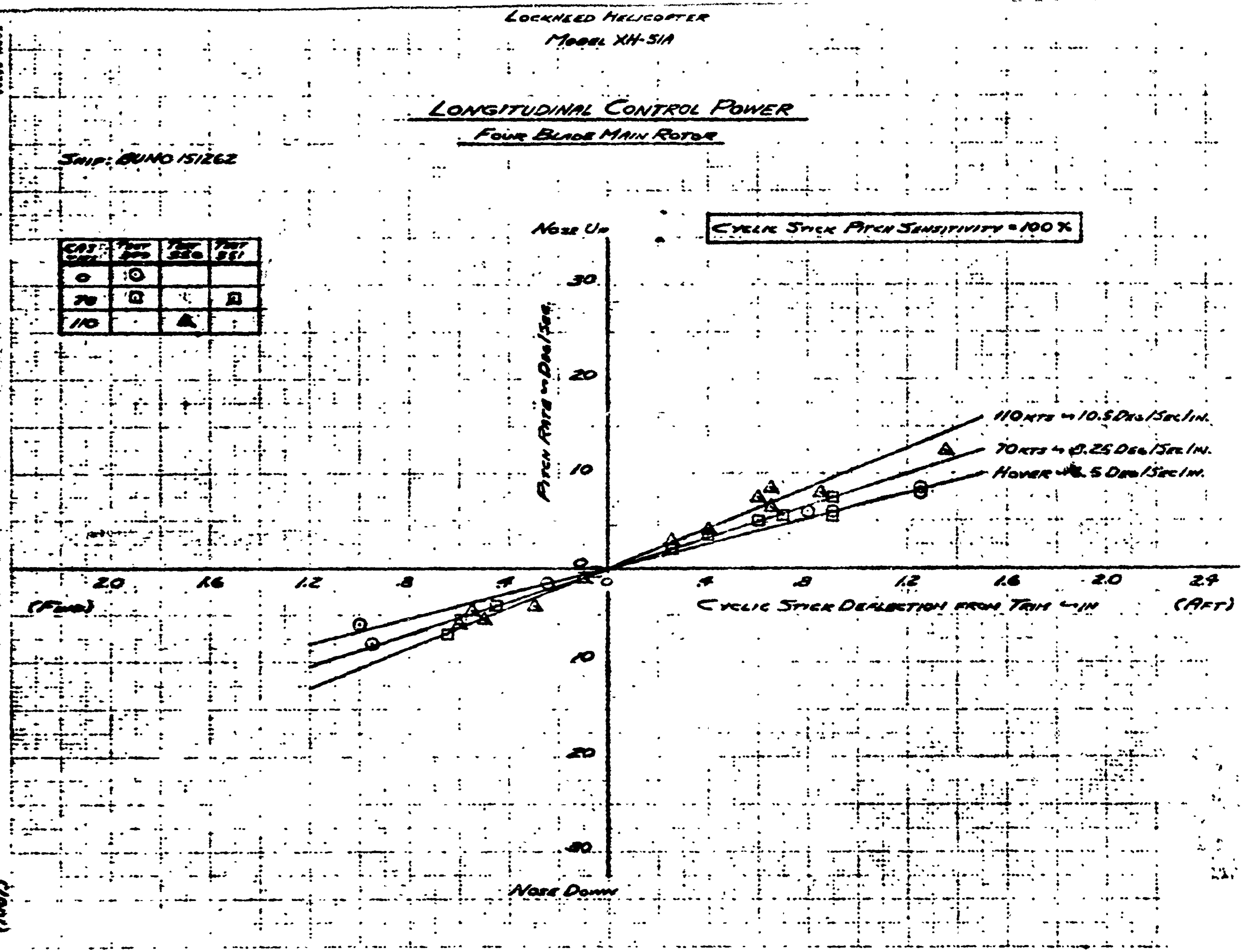

LONGITUDINAL CONTROL POWER

FIGURE 20

(1001)

979A

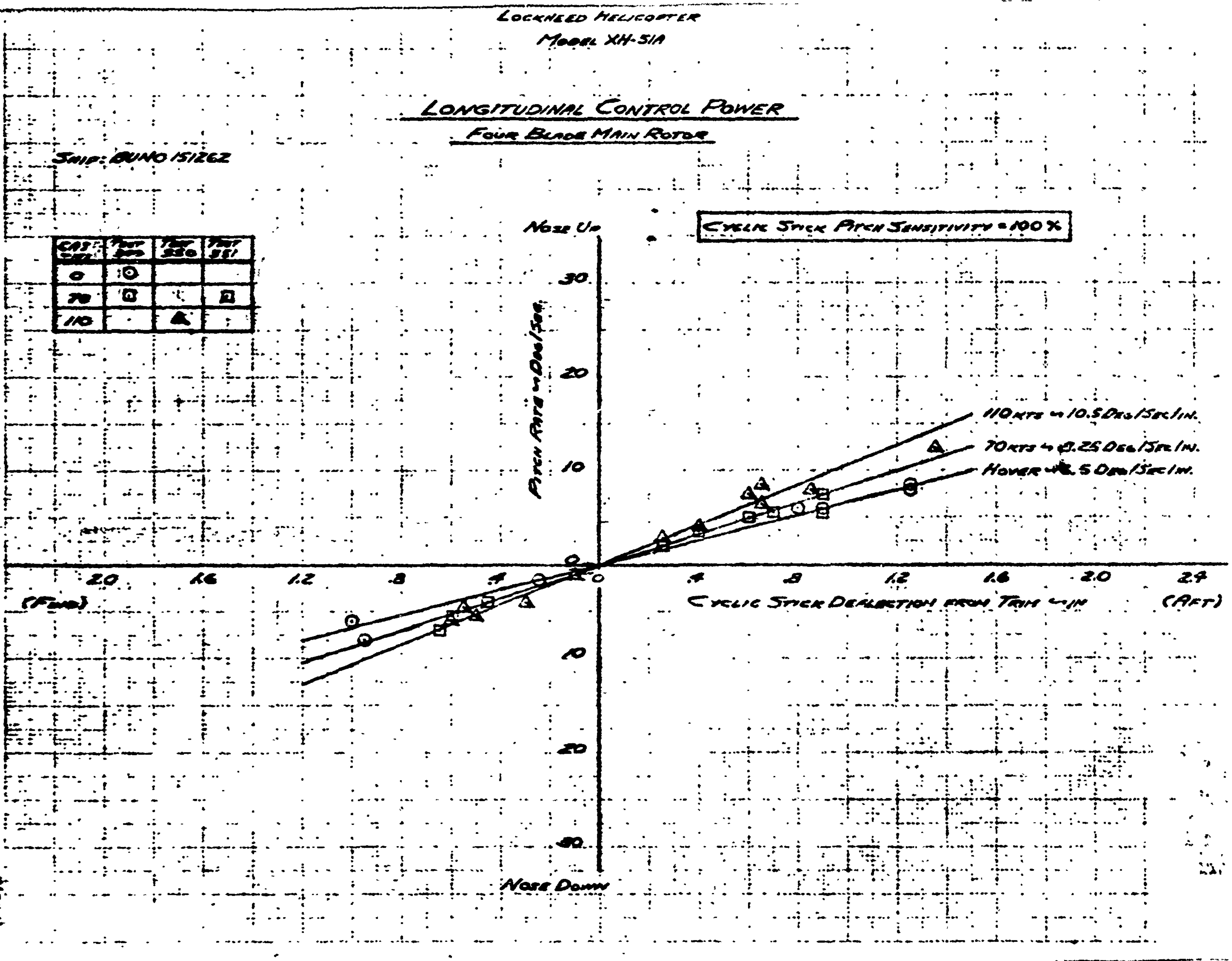

FORM 5570A

LONGITUDINAL CONTROL POWER

FIGURE 20

(1001)

979A

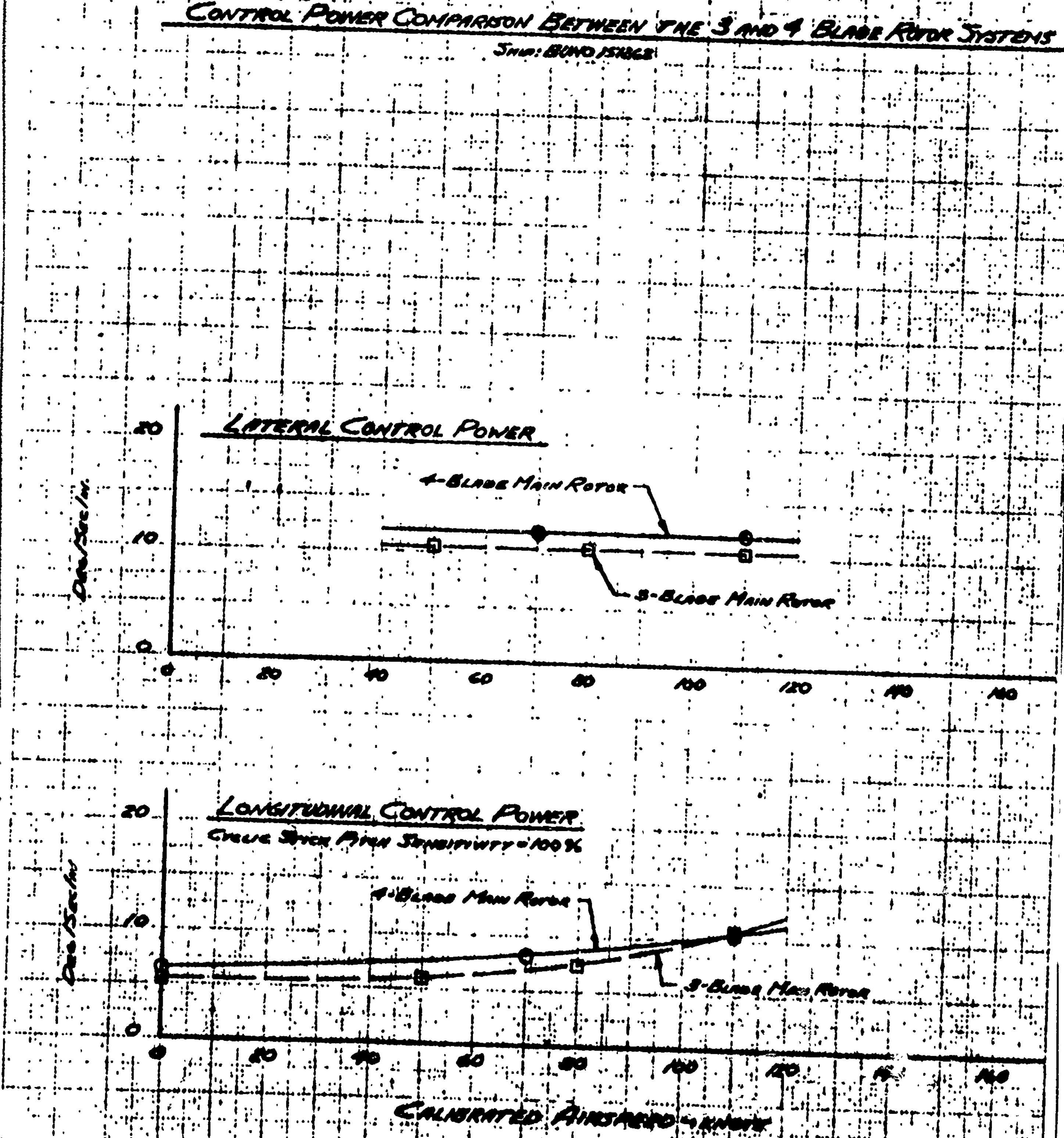

FORM 8879A

CONTROL POWER COMPARISON — 3 BLADE & 4 BLADE ROTORS

FIGURE 22

CONTROL POWER COMPARISON BETWEEN THE 3 AND 4 BLADE ROTOR SYSTEMS

SHIP: BUNO 151862

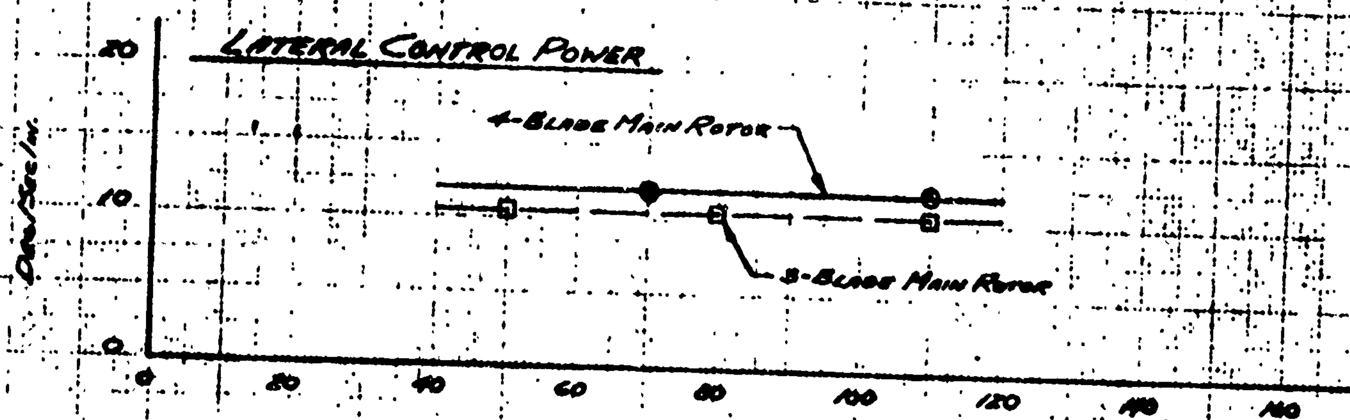

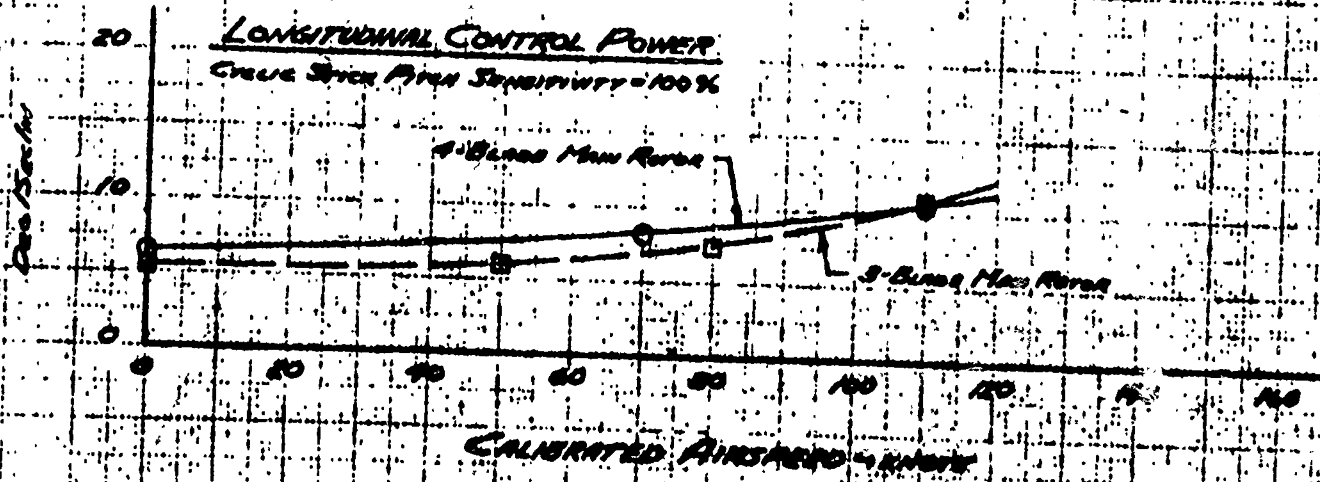

FORM 5379A

CONTROL POWER COMPARISON — 3 BLADE & 4 BLADE ROTORS

FIGURE 22

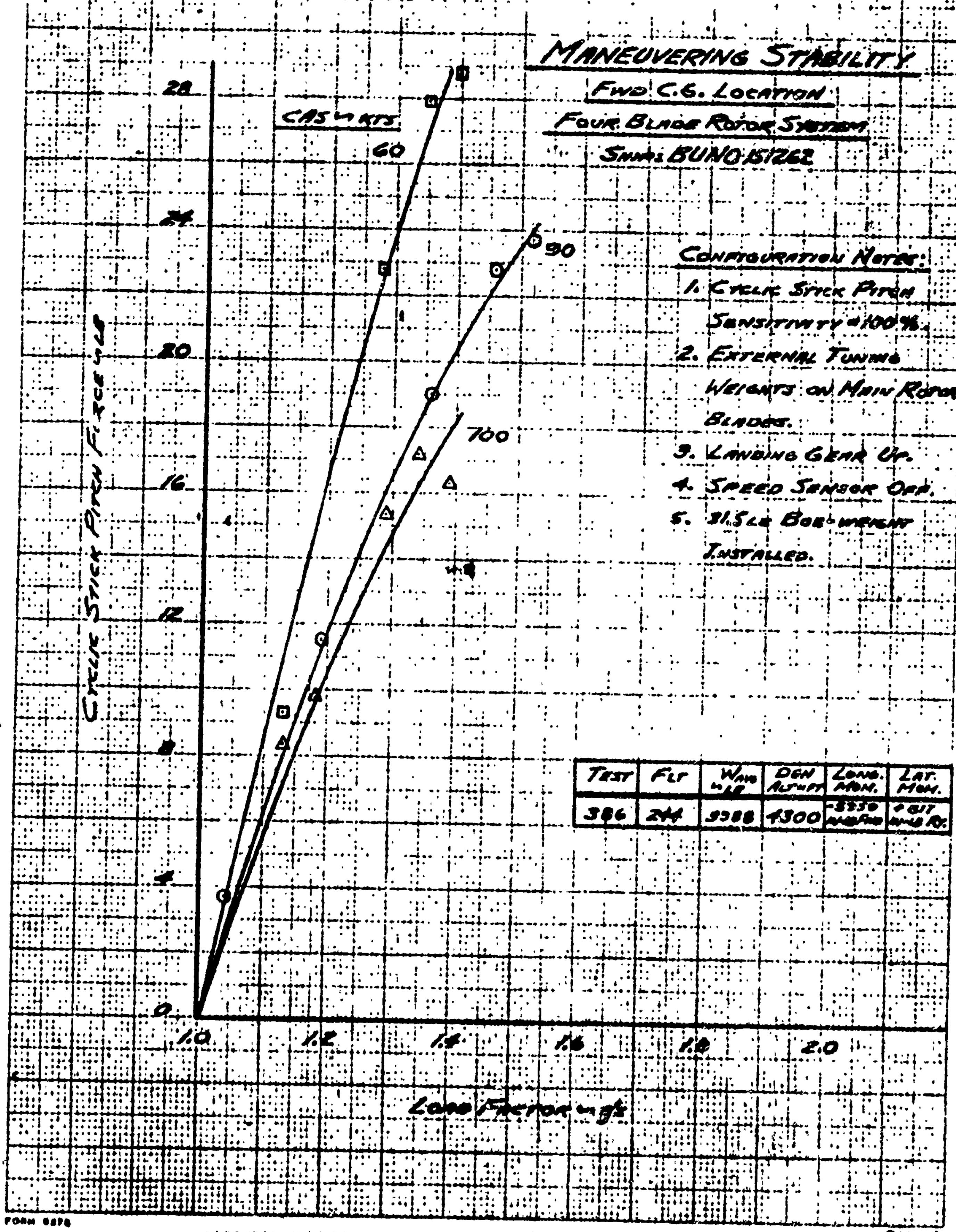

MANEUVERING STABILITY 4 BLADE SYSTEM

FIGURE 23

994A

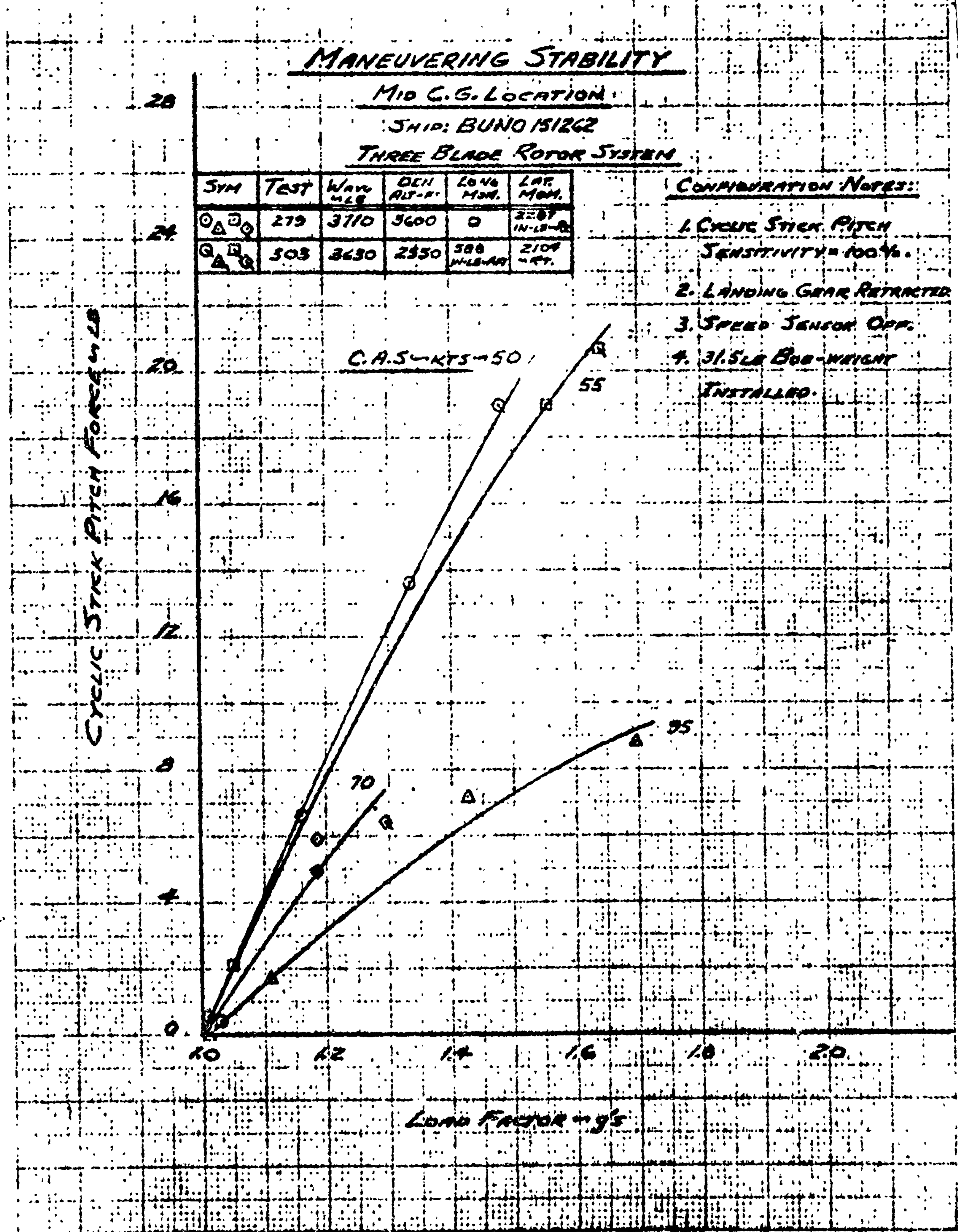

FORM 4276

MANEUVERING STABILITY 3 BLADE ROTOR
FIGURE 24

879A
(1001)

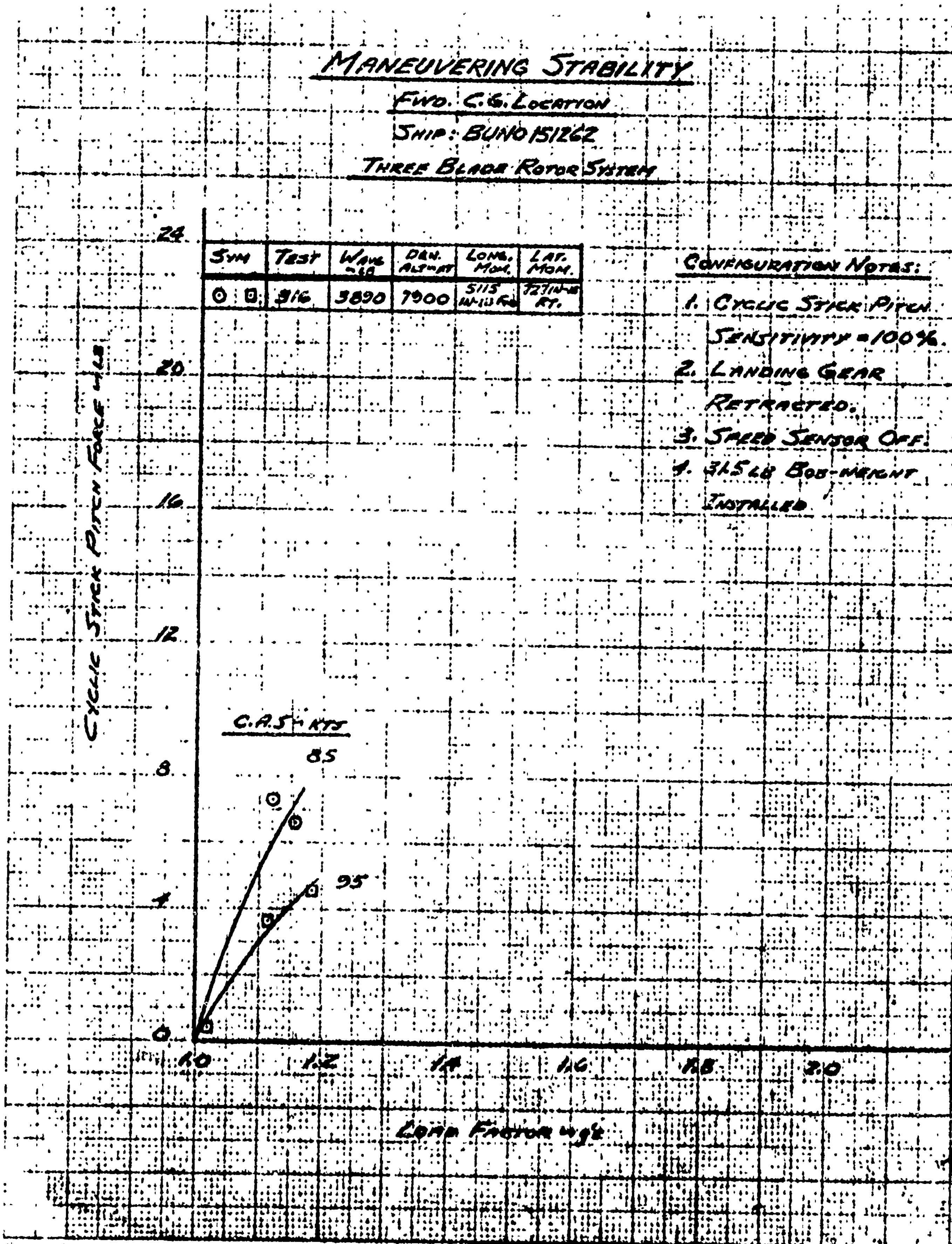

MANEUVERING STABILITY 3 BLADE ROTOR

FIGURE 25

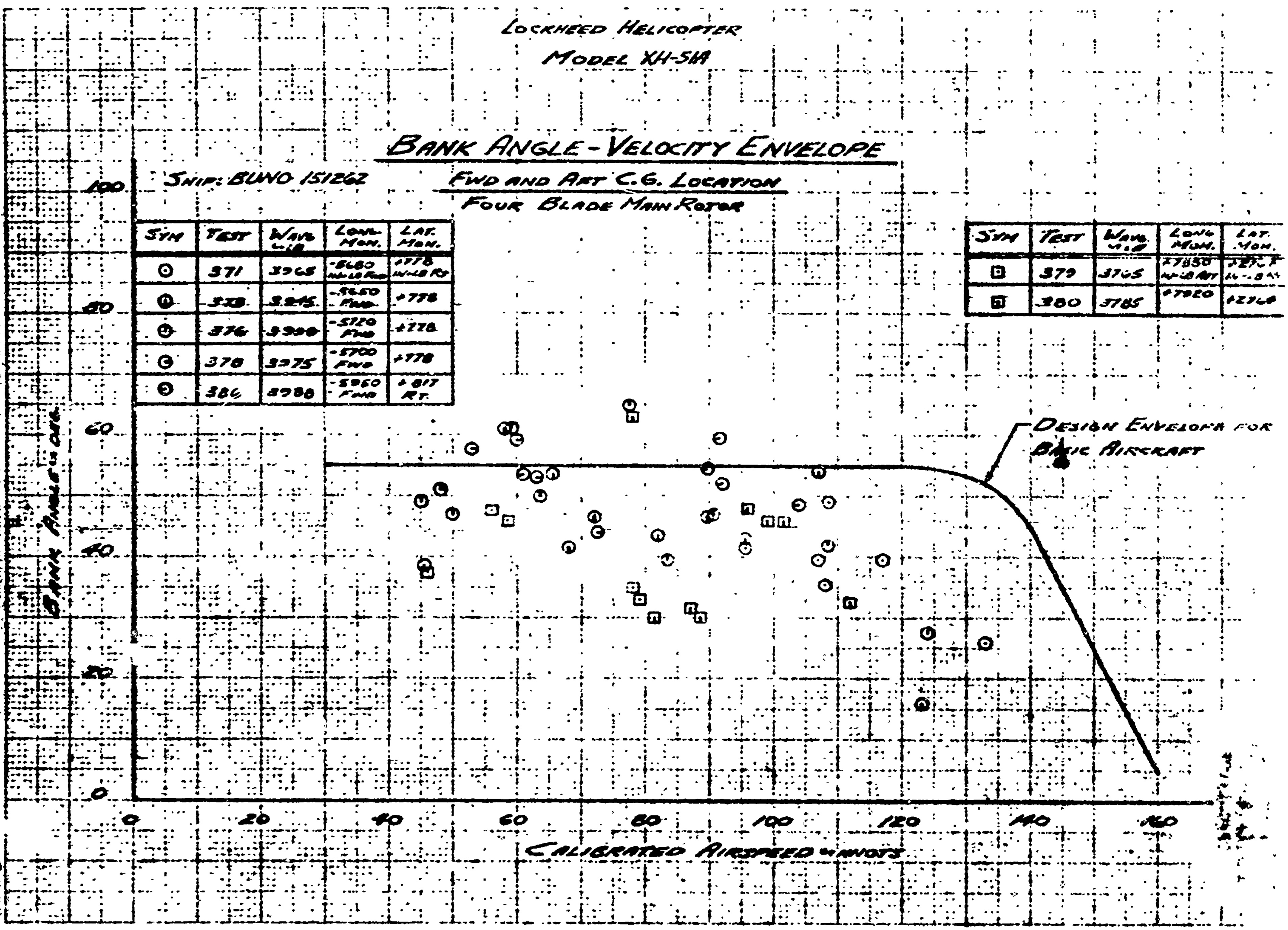

ANGLE OF BANK VELOCITY ENVELOPE

FIGURE 28

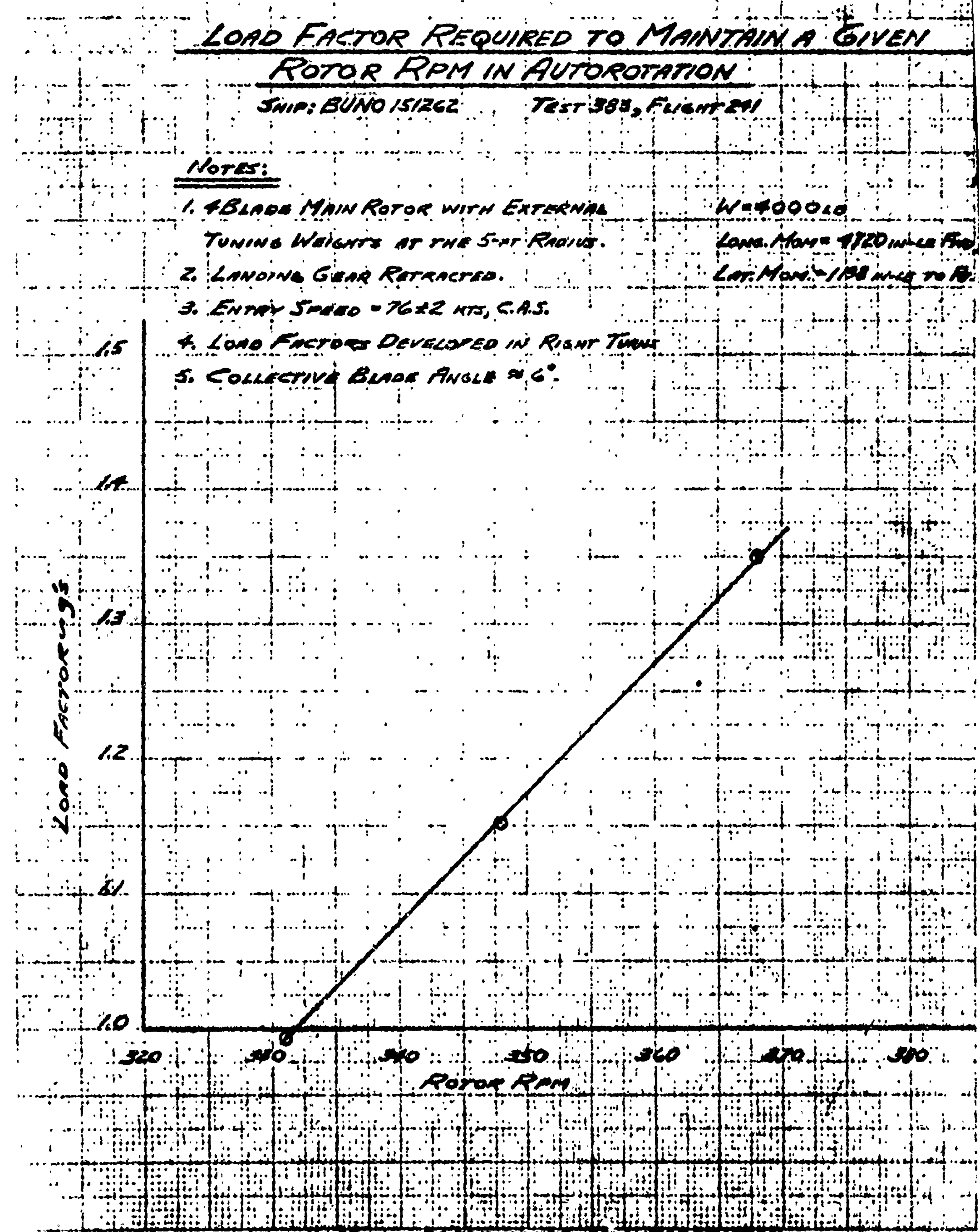

LOAD FACTOR – ROTOR SPEED IN AUTOROTATION (1001)

FIGURE 27

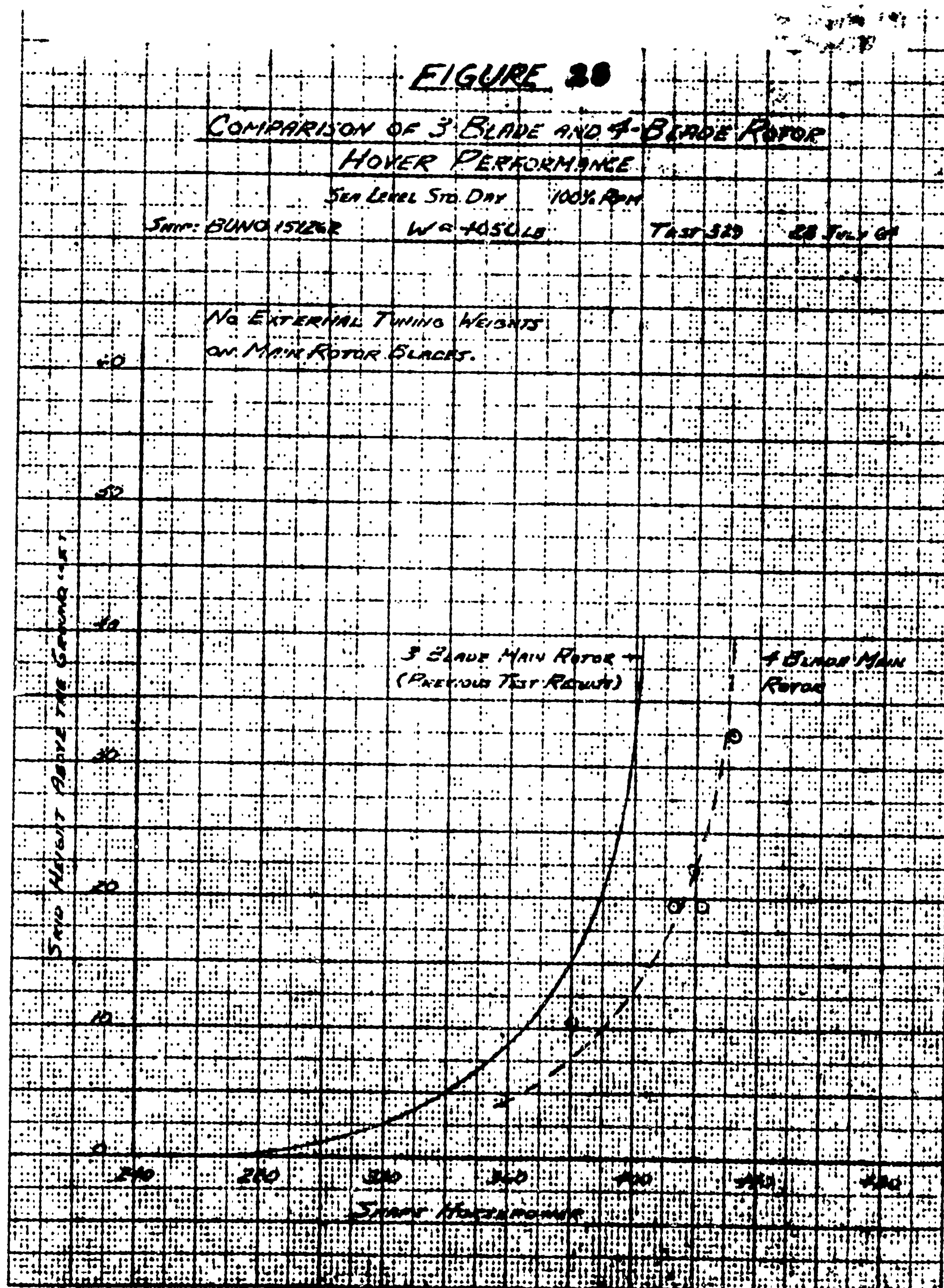

HOVER PERFORMANCE

FIGURE 28

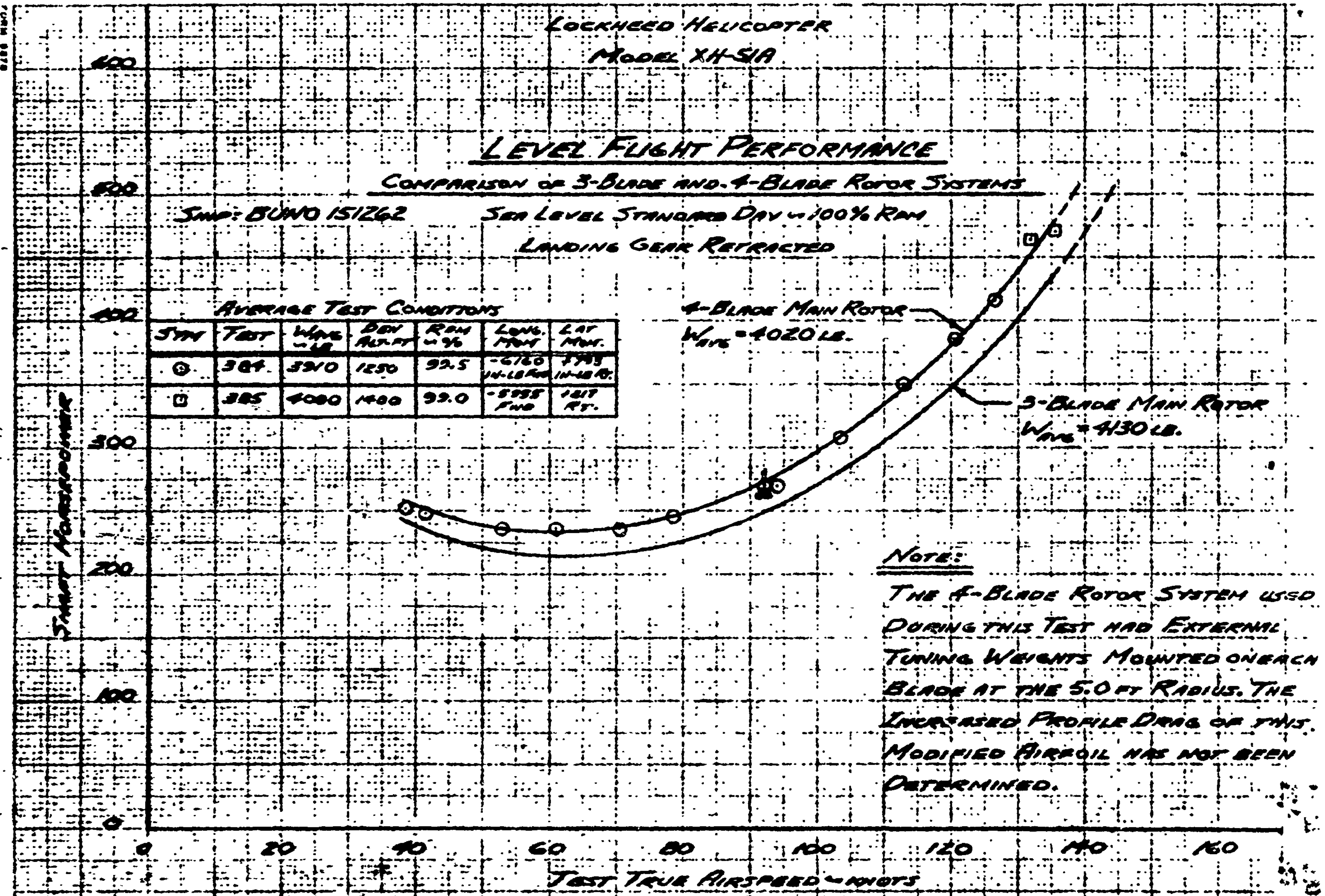

FORWARD FLIGHT PERFORMANCE

FIGURE 29